

**Response of *Polytrichum strictum* Plants to Regional Warming of the Antarctic Peninsula Using Geochemistry of Peat and Modern and Fossil Plants**

A THESIS SUBMITTED TO  
THE GLOBAL ENVIRONMENTAL SCIENCE  
UNDERGRADUATE DIVISION IN PARTIAL FULFILLMENT  
OF THE REQUIREMENTS FOR THE DEGREE OF

BACHELOR OF SCIENCE

IN

GLOBAL ENVIRONMENTAL SCIENCE

May 2016

By  
Lauren Yumol

Thesis Advisor

David Beilman

I certify that I have read this thesis and that, in my opinion, it is satisfactory in scope and quality as a thesis for the degree of Bachelor of Science in Global Environmental Science.

THESIS ADVISOR

---

David Beilman  
Department of Geography

*To my parents, Marc, Jasper, and my GES family.  
Thank you for all of your support throughout this journey, I could not have done this  
without you.*

## ACKNOWLEDGEMENTS

This project was made possible by the support of many colleagues, friends, and family. I would like to acknowledge and thank Dr. David Beilman for his guidance, patience, and outstanding motivational support. Having the opportunity to learn and gain lab and research experience from him has been a great pleasure and I can assure that my abilities are substantial because of him. I would like to thank everyone in the Biogeochemical Stable Isotope Facility for analyzing many of my samples and for always getting results back to us as quick as possible. A special thanks to Alex Hedgpeth at CAMS Laurence Livermore National Laboratory for not only processing my radiocarbon samples, but for also being a great mentor and role model to me during your time working in the Beilman lab. To the entire Beilman lab: Olivia Marohnic, Charly Massa, Mary Tardona, and Olivia Schubert, thank you for your advice and support over the last year and a half. I would also like to thank our colleagues at Lehigh University for their contribution and input to the entire Antarctic project, the Undergraduate research opportunity program, and the National Science Foundation for providing the funding necessary to complete this project. Last but certainly not least, I would like to thank my GES family, Michael Guidry, Kristin Momohara, and Catalpa Kong, for always being there and for making my undergraduate career the best and most fulfilling.

## ABSTRACT

Ecosystems of the western Antarctic Peninsula (AP) are currently experiencing one of the fastest rates of regional warming in the world. Aerobic moss-dominated peatbanks, which have the most flourishing vegetation in this ice-dominated region, were studied along the wAP to investigate plant growth conditions over space and time. Living plants of the dominant moss bank species, *Polytrichum strictum*, were collected from 13 populations along seven sites located between 64°09' and 67°35'S and a core was raised from a *Polytrichum*-dominated moss bank at 65°14'S. Stable isotope ratios were measured in modern and fossil plant tissue. Modern plant  $\delta^{13}\text{C}$  values varied from  $-31.7$  to  $-27.0\text{‰}$  and were influenced more by tissue type than geographic location. Modern plant  $\delta^{15}\text{N}$  values ranged from  $-1.4$  to  $+14.7\text{‰}$  showing little tissue effect. In the core, radiocarbon-dated fossil leaf tissue showed plant growth began 2300 years ago (one of the oldest plant ages on the wAP), peat accumulation rates varied over time, and there is evidence for a hiatus between  $\sim 1600$  and 800 years ago BP. Fossil leaves deposited during recent decades had  $\delta^{13}\text{C}$  values between  $-30.3$  and  $-27.2\text{‰}$  that were  $2.0\text{‰}$  more depleted than any time during the last 2300 years. Enriched  $\delta^{15}\text{N}$  values of  $+11.5$  to  $+13.2\text{‰}$  in fossil leaves deposited between 209 and 700 years before present (BP) suggest a period of more tropically-enriched animal inputs. Our results suggest *P. strictum* plants have experienced unprecedented growth conditions with recent rapid warming and that moss bank ecosystems may have changed nutrient sources over time.

## TABLE OF CONTENTS

Dedication.....	iii
Acknowledgements.....	iv
Abstract.....	v
List of Tables.....	vii
List of Figures.....	ix
List of Abbreviations.....	xi
1.0 Introduction.....	11
1.1 BACKGROUND.....	11
1.2 BRYOPHYTE SENSITIVITY TO ENVIRONMENTAL CHANGE.....	13
1.3 ISOTOPIC DISCRIMINATION AND CLIMATE.....	16
1.4 HISTORY OF PALEOENVIRONMENTAL STUDIES ON A.P.....	19
1.5 HYPOTHESES AND RESEARCH QUESTIONS.....	22
2.0 Methods.....	24
2.1 STUDY SITES AND SAMPLE COLLECTION.....	24
2.1.1 MODERN PLANT COLLECTION.....	24
2.1.2 CORE EXTRACTION.....	24
2.2 MODERN PLANTS STABLE ISOTOPE ANALYSES.....	25
2.3 BULK SEDIMENT CHARACTERISTICS.....	25
2.4 TERRESTRIAL MOSS BANK CORE.....	26
2.5 RADIOCARBON DATING AND ACCUMULATION RATES.....	26
2.6 CALCULATING MOSS DISCRIMINATION.....	27
3.0 Results.....	28
3.1 MODERN PLANT TISSUE.....	28
3.1.1 CARBON AND NITROGEN CONTENT.....	28
3.1.2 $\delta^{13}\text{C}$ VALUES.....	29
3.1.3 $\delta^{15}\text{N}$ VALUES.....	30
3.2 GALINDEZ ISLAND BULK SEDIMENT CORE.....	30
3.3 GALINDEZ ISLAND FOSSIL LEAF MATERIAL.....	31
3.3.1 ACIDIFIED VS. NON-ACIDIFIED TEST.....	31
3.3.2 $\delta^{13}\text{C}$ VALUES.....	32
3.3.3 $\delta^{15}\text{N}$ VALUES.....	33
3.4 RADIOCARBON AGE ESTIMATES.....	34
3.4.1 AGE-DEPTH MODEL.....	34
3.4.2 C, OM, DRY MASS ACCUMULATION RATES.....	36
4.0 DISCUSSION.....	38
4.1 MODERN PLANT TISSUE STABLE CARBON AND NITROGEN VARIATION.....	38
4.2 AGE-DEPTH MODEL HIATUS AND ACCUMULATION RATES.....	40
4.3 FOSSIL LEAF STABLE ISOTOPE VARIATION.....	41
5.0 CONCLUSION.....	45
APPENDIX.....	47
LITERATURE CITED.....	53

## LIST OF TABLES

Table 1. $^{14}\text{C}$ -AMS Data.....	35
Table 2. Modern Plant Data (Appendix A).....	47
Table 3. Bulk Sediment Data (Appendix B).....	48
Table 4. Fossil Leaf Data (Appendix C) .....	50

## LIST OF FIGURES

Figure 1. Annual and Spring Mean Temperatures.....	11
Figure 2. Map of Antarctic Peninsula.....	12
Figure 3. <i>P. strictum</i> Plant Physiology .....	16
a. <i>P. strictum</i> leaf.....	16
b. Cross Section of Stem.....	16
c. Cross Section of Leaf.....	16
Figure 4. South Pole Atmospheric CO <sub>2</sub> and δ <sup>13</sup> C Observations .....	19
Figure 5. Paleoenvironmental Proxies .....	20
a. Ice Shelf Extent.....	20
b. Sea Surface Temperature.....	20
Figure 6. Recent Sea Ice Extent and Annual Mean Air Temperature .....	21
Figure 7. Map of Sampling Sites .....	25
Figure 8. Stem and Leaf Data .....	31
Figure 9. Bulk Sediment Data.....	32
Figure 10. Acidified vs. Non-acidified Test .....	33
a. Carbon Content Results.....	33
b. δ <sup>13</sup> C Results.....	33
c. Nitrogen Content Results.....	33
d. δ <sup>15</sup> N Results.....	33
Figure 11. Fossil Lead Data.....	36
a. δ <sup>13</sup> C Values.....	36
b. δ <sup>15</sup> N Values.....	36



c. C:N Ratios.....	36
Figure 12. Radiocarbon Results.....	37
a. Age-Depth Curve.....	37
b. Sediment Accumulation Rates.....	37
Figure 13. Dry Mass, Carbon, and Organic Matter Accumulation Rates.....	37
Figure 14. Leaf-Stem Comparison.....	39
Figure 15. Stable isotope time-series.....	42
a. Fossil $\delta^{13}\text{C}$ values.....	42
b. Fossil $\delta^{15}\text{N}$ values.....	42
Figure 16. Source-independent discrimination comparisons.....	44
a. Source-independent discrimination of <i>P. strictum</i> mosses.....	44
b. Barilari Bay sea ice extent.....	44
c. Palmer Deep SST.....	44

## LIST OF ABBREVIATIONS

AP – Antarctic Peninsula

BP – Before present

C – Carbon

N – Nitrogen

$\delta^{13}\text{C}$  – Delta carbon-13 (‰ vs. PDB)

$\delta^{15}\text{N}$  – Delta nitrogen-15

RuBisCo – Bisphosphate carboxylase/oxygenase

$\text{NO}_x$  – Generic mono-nitrogen oxides term

$\text{NH}_y$  – Generic mono-nitrogen ammonium term

HCl – Hydrochloric acid

LOI – Loss on ignition

$^{14}\text{C}$  – Radiocarbon

OM – Organic matter

EA-IRMS – Elemental Analyzer-Isotope Ratio Mass Spectrometer

CAMS – Center for Accelerator Mass Spectrometry

C% – Carbon content as a percent

N% – Nitrogen content as a percent

TC% – Total carbon content measured as a percent from bulk sediment

TN% – Total nitrogen content measured as a percent from bulk sediment

MCMC – Markov Chain Monte Carlo

## 1.0 INTRODUCTION

### 1.1 BACKGROUND

Over the last 50 years, mean annual air temperatures, recorded from Faraday Station on the western Antarctic Peninsula (AP), have increased by almost  $+2.5^{\circ}\text{C}$ , making this region one of the fastest warming places in the world (Jones et al., 1993). Mean temperatures recorded from four stations along the western AP show temperatures have increased between 1950 to 2015 both annually and during the Spring growing season months (Figure 1). The warming rate of this region suggests that plant species will respond in order to adapt to these rapid climate changes. The Southern Hemisphere westerlies and the Antarctic Circumpolar Current are responsible for the maritime climate of the wAP, driving cold winters and cool summers (Turney et al., 2015). The maritime Antarctic is generally warmer and wetter than anywhere else on the continent allowing more diverse plant species to flourish (Day et al., 2008).

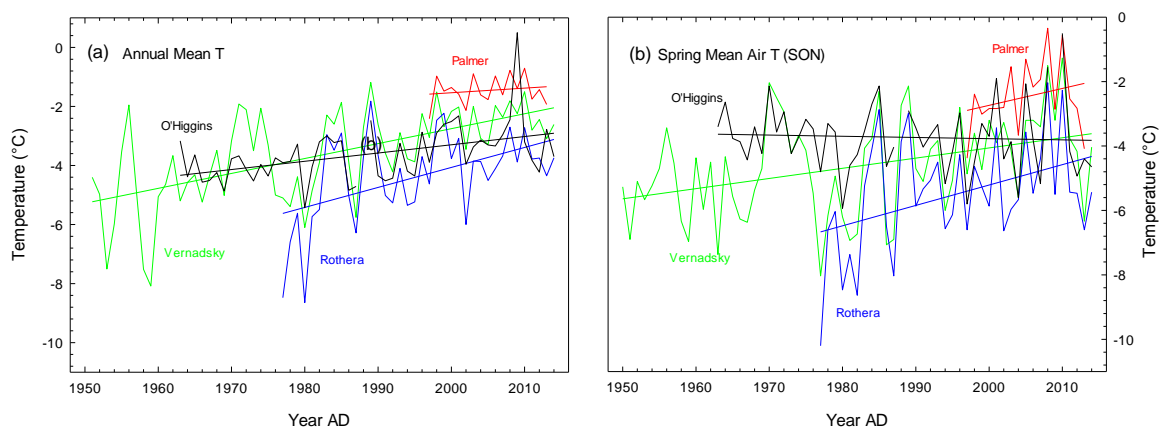


**Figure 1.** Mean air temperatures recorded from four stations along the Antarctic Peninsula from 1950 to 2015, **a)** annual mean temperature showing increasing temperatures at all four stations since 1950. **b)** Spring mean temperature during the early months of the growing season on the Antarctic Peninsula, showing increasing temperatures, particularly at Palmer, Vernadsky, and Rothera station. (Colwell 2009)

Plant biodiversity in the AP includes only two vascular plant species, *Deschampsia antarctica* and *Colobanthus quitensis*, but a diverse flora of lower plants including between 100-115 moss species and 350 species of lichens in the maritime Antarctic alone (Roberts et al., 2009; Peat et al., 2006). The plants of the AP are important components of carbon cycling processes such as primary production, respiration, and litter decomposition (Cannone et al., 2011). Ice-free areas, limited to less than 50,000 km<sup>2</sup> on Antarctica, provide natural environments for studying these carbon cycling processes as they are influenced by climate and other natural processes (Cannone et al., 2011). The growing season for terrestrial plants on the AP is relatively short lasting between 120 and 150 days during the late austral spring and summer periods when free water becomes available as a result of snow and ice melt (Beyer & Bolter 2002; Royles et al., 2012). The relatively short growing season of this polar environment is expected to

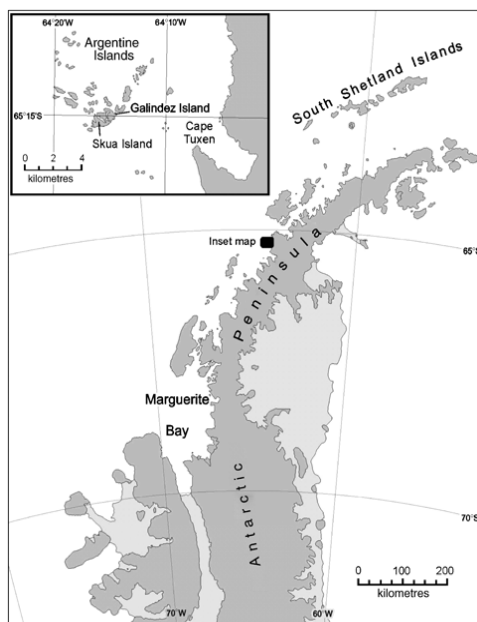


**Figure 2.** Map of the Antarctic Peninsula and map inset focusing on Galindez Island located on the western side of the Antarctic Peninsula. (Parnikoza et al., 2009)

lengthen as temperatures and ice-free area increases ultimately creating more ice- and snow-free days (Fenton & Smith 1982). Longer growing seasons provides better environmental conditions for plants to photosynthesize over longer periods of time potentially allowing organic matter to accumulate at faster rates and facilitating the ‘greening’ of the AP (Convey et al., 2011).

Typical climate conditions of the western AP support the accumulation of peat. Aerobic

peat banks, which dominate the western AP, form as a result of the imbalance between plant productivity and decomposition in which plant productivity at the surface exceeds decomposition (Moore et al., 1998; Charman 2002). The imbalance between primary productivity and decomposition is a characteristic of peat formation and carbon accumulation in wetlands overtime, making them important sinks of carbon (Clymo et al., 1998). Under the influence of climate change, there is a possibility of aerobic peat banks shifting from being a carbon sink to a potential carbon source to the atmosphere as increasing temperatures promote warmer soil temperatures (Royles et al., 2012; Cannone et al., 2012).

## **1.2 BRYOPHYTE SENSITIVITY TO ENVIRONMENTAL CHANGE**

The majority of the vegetation on western AP is dominated by turf forming bryophyte mosses and lichens (Peat et al., 2006). Bryophytes in particular are highly diverse land plants that survive in various habitats on every continent (Longton 1988). The main characteristics of bryophytes include liquid water being required to facilitate sexual reproduction, the absence of stomata in most moss species tissues, and the dominance of haploid gametophytes (Longton 1988). Bryophyte biomass in peat is a significant component of the global carbon cycle, and under the influence of climate change the carbon stored in peat has potential to be released to the atmosphere as CO<sub>2</sub> (Gorham 1991; Koven et al., 2011).

Fossil bryophytes that exist in cold polar environments are well preserved due to cold soil temperatures and even permafrost slowing down the rate of decomposition, which can promote peat accumulation (Gorham 1991). Using stratigraphic cores from polar peat banks to analyze stable isotope compositions of plant fossils can be an

effective method to evaluate important components of past and modern growing season conditions. Plant identification and separation is a key factor during the reconstruction process, as peat forming communities typically consist of more than one species and isotope values vary from one plant species to another.

*Polytrichum strictum* plants that grow on the western AP form thick aerobic moss banks at low elevations, from sea level to about 200-250 meters (Fenton & Smith 1982). The formation of these deep turf-like moss banks provide a cushion-like environment where plants can merge, eventually accumulating organic matter that can be up to 1-2 meters in depth (Smith & Bednarek-Ochyra 2008). The deep moss banks that form in the maritime Antarctic are composed primarily of two dominating moss species, *P. strictum* and *Chorisodontium aciphyllum* (Fenton & Smith 1982). Peat that is composed of *P. strictum* is distinct from that composed of *C. aciphyllum* in its physical structure, which is denser and more compact (Fenton & Smith 1982). The *P. strictum* plants that grow on the surface of the moss peat banks are sturdy and resistant to wind erosion because of the structure of the shoots, which are bound together by dense tomentum of rhizoids (Figure 3b, Fenton & Smith 1982). Previous ecological studies done in the Arctic region have observed a sparse population of *P. strictum* plants, as they are typically outcompeted by more dominating *Sphagnum* species (Bu et al., 2010), whereas *Sphagnum* is absent from Antarctica (Longton 1988).

*P. strictum* mosses are non-vascular plants that do not have stomata in their leafy gametophyte (Peat et al., 2007). However, *Polytrichum* mosses are considered endohydric in that they conduct water from the base of their plant where it enters water conducting cells called hydroids (Figure 3b, Peat et al., 2007). In general, mosses are

poikilohydric in that they are unable to internally regulate water and are restricted to utilizing water that is available in their immediate environment (Stuber 2013).

Additionally, being poikilohydric means when there are wet environmental conditions, the plants are wet, when conditions are dry, the plants are dry (Stuber 2013), making for a close association between weather and growth. However, the leaves of *P. strictum* plants contain a unique feature that allows them to avoid desiccation by utilizing water vapor in the air (Proctor 2005).

The leaves of *Polytrichum* plants differentiate themselves from any other moss species by possessing photosynthetic lamellae on the upper surface of their leaves (Figure 3a, 3c, Proctor 2005). This characteristic of tissue leaf tissue increases the surface area which increases the photosynthetic rate of the plant (Thomas et al., 1996). Lamellae in *Polytrichum* plant leaves allow humid air to get trapped by thick-walled cells which are used to protect the tissue beneath providing minimal water loss (Silverside 2010). When environmental conditions are dry, *Polytrichum* plant leaves curve and twist around the stem in order to avoid water loss (Silverside 2010). The photosynthetic efficiency of *Polytrichum* plants is a result of these mosses bearing rows of surface lamellae in their leaves, a characteristic that enables the moss to facilitate diffusion of CO<sub>2</sub> into the leaf faster compared to most other mosses (Krupa 1984). When climate conditions are dry and leaf lamellae are less exposed to air, being endohydric provides *P. strictum* with the capacity for internal water transport which enables tissues to avoid desiccation (Bu et al., 2011). Despite *Polytrichum* leaves possessing photosynthetic lamellae and a rigid leaf center, the transport mechanisms used to deliver water and CO<sub>2</sub> from the leaf to the stem are limited to the internal region of the leaf (Thomas et al., 1996).

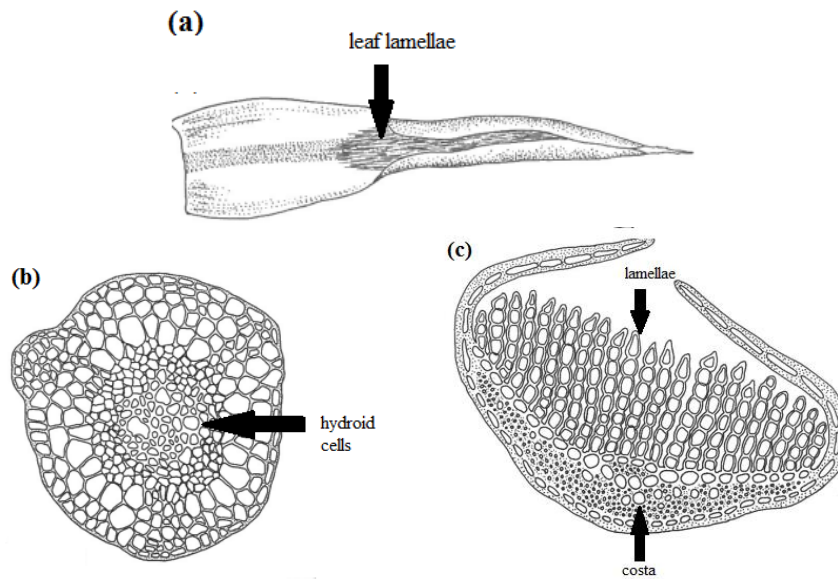


**Figure 3.** *Polytrichum* leaf physiology showing **a)** *P. strictum* leaf with arrow labelling leaf lamellae. **b)** cross section of stem arrow indicating the location of stem hydroid cells and **c)** a cross section of a leaf with the lamellae and costa where the leaf hydroids exist for water transport (Ochyra et al., 2008)

### 1.3 ISOTOPIC DISCRIMINATION AND CLIMATE

As terrestrial plants photosynthesize, their physiological responses to environmental changes can be partly understood using geochemical techniques. The value of modern and fossil plant tissue carbon (C) and nitrogen (N) stable isotope ratios reflect the environmental conditions during the time of tissue biosynthesis (Gavazov et al., 2015). Stable C isotopes measured from plant tissue are analyzed to represent the exchange amongst plant C and water, which is a useful way to determine how a plant functions (Dawson et al., 2002). Plants in general discriminate against the heavier C isotope,  $^{13}\text{C}$ , due to the favored assimilation of the lighter  $^{12}\text{C}$  isotope by the carboxylating enzyme, bisphosphate carboxylase/oxygenase or RuBisCo, when photosynthesis takes place (Farquhar et al., 1989; Dawson et al., 2002).

The assimilation of  $^{12}\text{C}$  by RuBisCo is an example of a kinetic isotope effect that creates variation in the  $^{13}\text{C}/^{12}\text{C}$  ratio (Farquhar et al., 1989). This ratio compares the



heavier carbon isotope to the lighter isotope,  $^{13}\text{C}/^{12}\text{C}$ , to express the isotopic signature of a material and isotope effects cause variation in the ratio (Farquhar et al., 1989). The mass spectrometer is used to measure the deviation of the isotopic composition of the material from a standard and is represented by  $\delta$ . The isotopic composition of a material is calculated by the following equation

$$\delta^x E = 1000 \times \left( \frac{R_{\text{sample}}}{R_{\text{standard}}} - 1 \right)$$

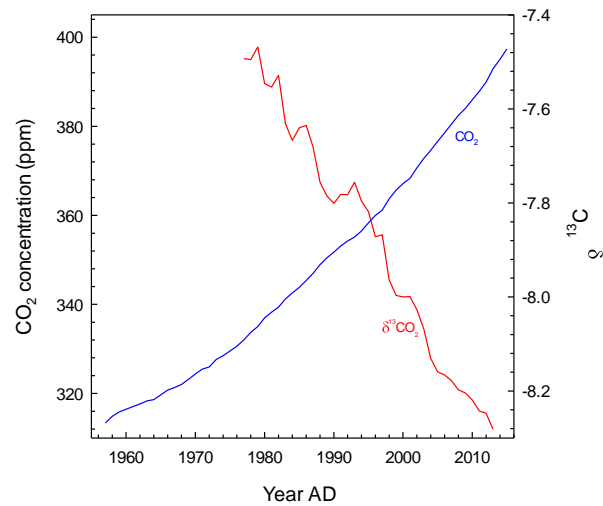
where “ $E$ ” is the element being analyzed ( $\delta^{13}\text{C}$  and  $\delta^{15}\text{N}$ ), “ $x$ ” is the mass of the heavier isotope in the abundance ratio, and  $R_{\text{standard}}$  is the molar abundance ratio ( $^{13}\text{C}/^{12}\text{C}$ ,  $^{15}\text{N}/^{14}\text{N}$ ) of the standard (Farquhar et al., 1989; Dawson et al., 2002). The entire equation is multiplied by 1000 so the final  $\delta$  value is in per mil units (‰). Enriched  $\delta^{13}\text{C}$  values are associated with plant respiration, which is a typical mechanism plants undergo when no photosynthesis is taking place (Park & Day 2007). In contrast, when photosynthesis is taking place the  $\delta^{13}\text{C}$  value of the plant will be increasingly depleted, as the plant will preferentially assimilate the lighter  $^{12}\text{C}$  isotope (Dawson et al., 2002).

In comparison to  $\delta$ , the total discrimination by the plant is represented as  $\Delta$ , and is the absolute isotopic discrimination independent of the isotopic composition of the substrate, also known as source independent discrimination (Farquhar et al., 1989). Calculating the source independent discrimination made by a plant is necessary to express the discrimination made by biological processes without influence of changes in of source isotopic value (Farquhar et al., 1989). The increasingly depleted trend in atmospheric  $\delta^{13}\text{C}\text{O}_2$ , which is the result of excessive anthropogenic fossil fuel burning also known as the “Suess effect”, can affect the  $\delta^{13}\text{C}$  values measured in a material and is

the reason calculating the source independent discrimination is an important step to assure the discrimination made by plants is free of atmospheric influence (Farquhar et al., 1989).

Plant tissue  $\delta^{15}\text{N}$  values are affected by a combination of factors including the presence of multiple N sources (i.e. animal inputs, anthropogenic sources), and dry and wet nitrogen deposition (Zechmeister et al., 2008). Anthropogenic atmospheric N inputs are low in Antarctica compared to areas in the Northern Hemisphere where N depositions are a result of human activities, so  $\delta^{15}\text{N}$  values of Antarctic plants should reflect more clearly changes in natural N sources (Lee et al., 2009). The discrimination of the stable  $^{15}\text{N}$  isotope made by plants measures the quality and quantity of N that is available and like  $\delta^{13}\text{C}$ ,  $\delta$  reports the deviation of the isotopic composition of the material from a standard and can be calculated using the equation on page 19 (Dawson et al., 2002). Enriched or depleted  $\delta^{15}\text{N}$  values measured from a plant or sediment is thus useful when interpreting N sources. For example, organic material containing  $\text{NO}_x$  forms of N tend to have more enriched  $\delta^{15}\text{N}$  signatures compared to that of  $\text{NH}_y$  compounds, which in turn tend to have more depleted  $\delta^{15}\text{N}$  signatures (Zechmeister et al., 2008). Sources of N inputs on the western AP are mainly derived from atmospheric deposition or animal inputs (Lee et al., 2009). Geochemical measurements of trace metals in bulk sediment can be analyzed to determine the difference between these N sources since the presence of certain metals such as, cadmium, can be associated with bird inputs (Zechmeister et al., 2008).

**Figure 4.** Average monthly atmospheric CO<sub>2</sub> concentrations increasing between the year 1957 to 2015 (blue) and average monthly atmospheric δ<sup>13</sup>CO<sub>2</sub> data showing concentrations are becoming more negative from 1977 to 2013 (red). Both data measurements were taken from the South Pole station located at the Southern-most point in Antarctica. (Keeling et al., 2016)



#### 1.4 HISTORY OF PALEOENVIRONMENTAL STUDIES ON A.P.

The recent rapid warming of the AP is unprecedented in the Holocene history and is associated with shifts in reduced duration of winter sea ice cover, disintegration of ice shelves, and the retreat of continental glaciers (Etouneau et al., 2013; Barbara et al., 2015; Bentley et al., 2007). Holocene paleoclimate records from the AP show variability in timing and extent of climate signal with two warm periods documented during the early- and mid-Holocene (Etouneau et al., 2013). Reconstructions of glacial ice fluctuations during the early Holocene reported an increasing retreat between 11,500 and 9000 yr BP, which agrees with Shevenell's (2011) SST reconstruction data reporting warming events during the same time period (Shevenell et al. 2011; Etouneau et al., 2015; Mulvaney et al., 2012).

Following a relative cooling of ~1°C that occurred between ~9200 and 5000 yr BP, slightly warmer temperatures were recorded during the Mid-Holocene between ~5000 to 3000 yr BP, and finally a second gradual cooling of ~1°C during the late Holocene (Etouneau et al., 2015). Ice records from the late Holocene provided evidence

to support the Little Ice Age impacted AP with climatic cooling and glacial advance between ~730 and 82 cal. yr BP and is associated with a decrease in sea surface temperatures (Figure 5a, 5b, Etouneau et al., 2015; Shevenell et al., 2011). During the last 2100 yr BP the western AP experienced a major climatic change characterized by a longer sea ice season and warmer sea surface temperatures during the summer (Figure 5b, Etouneau et al., 2013).

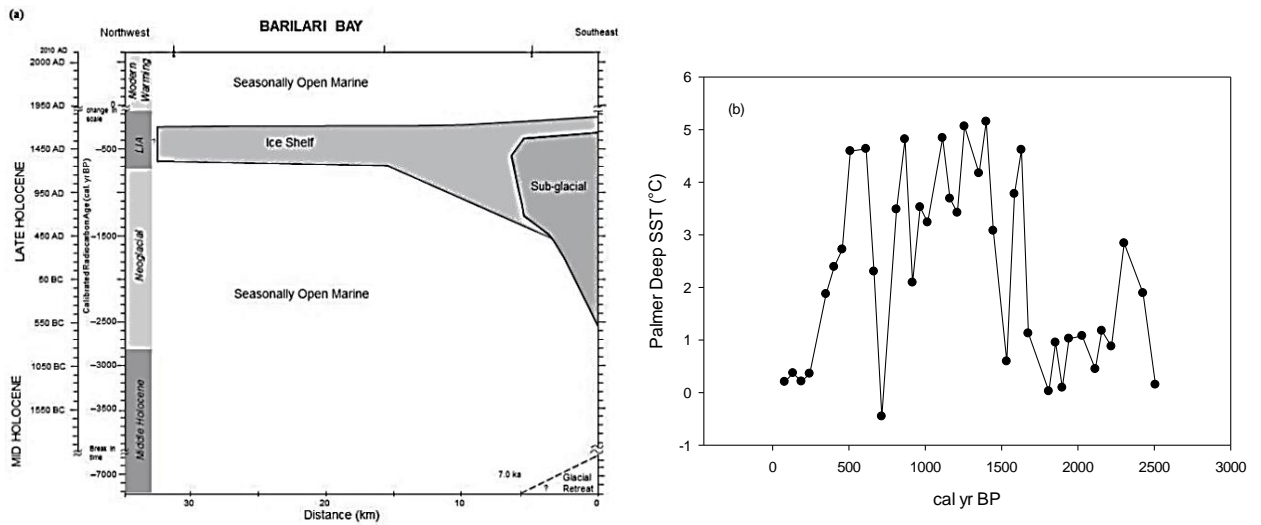


**Figure 5. a)** Space-time diagram highlighting the time period of the ice shelf extent during the Little Ice Age. Maximum extent of ice was recorded from ~730 to 82 cal. yr BP (Christ et al., 2014). **b)** Sea surface temperatures over the last 2500 cal. yr BP, indicating a significant period of warmer temperatures between ~1600 and 700 cal yr BP (Shevenell et al., 2011).

Seasonal variability of sea ice in most recent decades (since ~1980) shows an inverse relationship related to the seasonal cycle of air temperature until the late 1990's (Figure 6). From the late 1990's till present day, increased variability in mean annual air temperature is not associated with an anti-correlated response in sea-ice extent which may be linked to variability in large scale Earth processes such as El Nino-Southern Oscillation (ENSO, Smith et al., 2003).

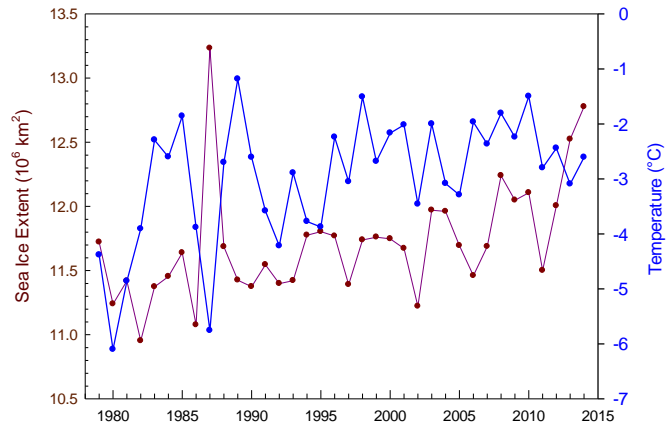


**Figure 6.** Mean variability in sea ice extent (dark red) from 1979 to 2014 showing an inverse relationship with mean annual sea surface temperature (blue) from 1982 till around 2002. Between 2002 and 2014, increasing sea ice extent is associated with an increase in temperatures. (Shevenell et al., 2011)

## 1.5 RESEARCH QUESTIONS and HYPOTHESES

This study will address the following questions:

- 1a. What variation is observed from stable carbon and nitrogen values of modern *P. strictum* populations at several sites along the Antarctic Peninsula?
- b. Can we observe any tissue effects that can be explained by recent climate warming in the stable carbon and nitrogen isotopes of modern *P. strictum* plants?
2. How has the dominant moss species, *Polytrichum strictum*, responded to environmental variation over the last 2290 years and how do fossil leaf stable isotope values compare to modern values?

Hypotheses:

1. Modern *P. strictum* plant populations will show variation in their tissue stable C isotope signatures based on geographic location showing more enriched  $\delta^{13}\text{C}$  values at southern sites and more depleted  $\delta^{13}\text{C}$  values in northern sites because temperatures decrease with increasing latitude (more south), with the understanding that plants show more depleted  $\delta^{13}\text{C}$  values when temperatures are warmer. Variation will be observed in the  $\delta^{15}\text{N}$  values of modern *P. strictum* plant tissue between sites with little or no trends displayed from latitudinal changes as a result of variations in amounts of animal deposits and/or atmospheric deposition varies at each site. Small differences will be seen in stem and leaf  $\delta^{13}\text{C}$  values as a result of biomolecular differences and little to no difference will be

seen in their  $\delta^{15}\text{N}$  values because the limited N that is available will be utilized and allocated to the entire plant.

2. Over time, the leaves of *P. strictum* plants are expected to display variations in both  $\delta^{13}\text{C}$  and  $\delta^{15}\text{N}$  signatures over the last 2290 years, with more discrimination of  $\delta^{13}\text{C}$  occurring during past climate warming shifts and in most recent decades as a result of temperatures increasing.

## **2.0 METHODS**

### **2.1 STUDY SITES AND SAMPLE COLLECTION**

#### ***1. Modern Plant Collection***

Modern plant samples were collected during cruise G-094-P in March of 2014, from 13 populations along the western AP. The plant samples were collected between 64°09'S 60°57'W to 67°35'S 68°21'W (Figure 7), and were used to analyze spatial differences amongst *P. strictum* plants. These modern plants were separated into stem and leaf tissue with assistance of a 0.65 magnification stereomicroscope. Moss tissues were analyzed separately to identify tissue-specific differences and responses to climate conditions.

#### ***2. Core Extraction***

To measure responses of *P. strictum* plants over time, a 55 cm terrestrial peat core was collected from a *P. strictum* dominated peat bank on Galindez Island (65°14'S 64°15'W) in March 2014. The core was raised using a box corer for active layer and a power-driven diamond-tipped drill for permafrost sections of the peat deposit that was stored in a -30°C freezer until the start of this study began in January 2015.



## 2.2 MODERN PLANTS STABLE ISOTOPE ANALYSES

The separated stems and leaves of modern living *P. strictum* plants mentioned in section 2.1.1 were analyzed for their stable carbon and nitrogen isotopes and carbon and

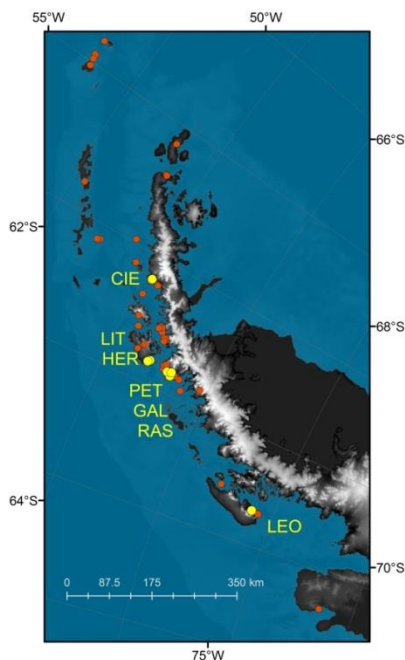


**Figure 7.** Map of the western Antarctic Peninsula, showing locations of the seven sampling sites referred to in the text (in yellow).

nitrogen content. Prior to being analyzed, a standard acid wash which entailed the tissues to be immersed in a 1N hydrochloric acid (HCl) wash for 30 minutes at 70°C in order to remove carbonates from the samples. Four water rinses were made using deionized 18.0 MΩ water until a neutral pH was achieved. The pretreated tissue samples were placed into glass vials and put in the drying oven to dry for 12 hours at 65°C. Once dried, ~2.5 mg of stems and leaves were individually weighed out into tin capsules and packaged for analysis by elemental analyzer-isotope ratio mass spectrometer (EA-IRMS) at the Isotope

Biogeochemistry Laboratory at the University of Hawaii at Manoa. The analytical precision of the isotopic measurements was  $< \pm 0.2\text{‰}$ . Statistics were calculated using Excel data analysis software.

## 2.3 BULK SEDIMENT CHARACTERISTICS

The core was split, and one half was sliced into contiguous one cm intervals using a band saw with stainless steel blade. Known-volume subsamples of an average  $1.6 \text{ cm}^{-3}$  were dried at 70°C for 24 hours to determine dry bulk density. Dried samples were then homogenized using a Retsch MM200 and passed through a 250-micron screen.

Subsamples of ~2000 mg of powdered peat were ashed at 550°C to determine organic matter (OM) content using the loss on ignition (L.O.I.) method (Robertson 2011).

Subsamples of an average 2.3 mg were loaded into tin capsules and measured for C and N elemental content and  $\delta^{13}\text{C}$  using Costech 4010 Elemental Analyzer and a Picarro G2201-i Cavity Ring-down Spectrometer at the University of Hawaii at Manoa.

## **2.4 TERRESTRIAL MOSS BANK CORE**

A 14.3 to 28.9 cm<sup>-3</sup> subsample from each continuous one cm section of the core ( $n=55$ ) was dispersed in 18.0M $\Omega$  water and dissected under a binocular microscope for *P. strictum* plants. Individual leaves were isolated from each plant found on every level of the core and acid washed, dried, weighed, and packaged in tin capsules using the same procedures described in section 2.2 and were analyzed by EA-IRMS at the Isotope Biogeochemistry Lab at the University of Hawaii at Manoa.

## **2.5 RADIOCARBON DATING AND ACCUMULATION RATES**

Four intervals chosen along the length of the core were sampled and individual *P. strictum* leaves were dissected from the peat matrix under a binocular microscope. The leaves of the *P. strictum* plants were removed to be used for high-density radiocarbon dating. To eliminate carbonates, organic acids, and other impurities each sample was treated with a standard “acid-base-acid” pretreatment which followed by multiple water washes until a neutral pH was achieved. The pretreated samples were weighed and put into premade quartz tubes. Once the samples were combusted, graphitized, and sealed, they were analyzed at the Center for Accelerator Mass Spectrometry (CAMS) at the Lawrence Livermore National Laboratory. The radiocarbon (<sup>14</sup>C) ages received from CAMS were calibrated using the software, CALIB 7.0.4, along with the Southern

Hemisphere dataset (Stuiver et al., 1998). The calibrated  $^{14}\text{C}$  dates and their corresponding sampling depths were used to determine the relationship between age and core depth using the Bayesian age-depth modelling software, BACON (Blaauw, 2010).

Sedimentation, dry mass accumulation, OM accumulation, and C accumulation rates were calculated using calibrated radiocarbon dates. Sedimentation rates were calculated in centimeters per year by taking the inverse of the difference between the age of the top of one slice and the age of the bottom of the slice. Bulk density values were then multiplied by the sedimentation rate, OM content and C content to determine the dry mass accumulation, OM accumulation and C accumulation rates.

## 2.6 CALCULATING MOSS DISCRIMINATION ( $\Delta$ )

Dated *P. strictum* leaves and the carbon isotope composition of past atmospheric  $\delta^{13}\text{CO}_2$  was used to calculate the carbon isotope discrimination ( $\Delta$ ) over time. The C isotope fractionation that occurs when a moss photosynthesizes was described by Farquhar *et al.* (1989) and is obtained from air and plant  $\delta$  values. The expression for the discrimination in leaves of  $\text{C}_3$  plants is,

$$\Delta = \frac{\delta^{13}\text{C}_a - \delta^{13}\text{C}_c}{1 + \delta^{13}\text{C}_c}$$

where  $\delta^{13}\text{C}_a$  and  $\delta^{13}\text{C}_c$  is the atmospheric isotopic composition of  $\text{CO}_2$  and the measured  $\delta^{13}\text{C}$  values of the plant, respectively (Farquhar et al., 1989). This equation was used in this study to determine the source independent discrimination made by *P. strictum* moss plants to explain the variation in  $\delta^{13}\text{C}$  measurements made using moss leaves derived from every centimeter of the Galindez Island core.

## 3.0 RESULTS

### 3.1 MODERN PLANT TISSUE

#### 3.1.1 CARBON AND NITROGEN CONTENT

Tissue results of the stems and leaves from modern *P. strictum* plants showed no trends between geographic locations from northern most sites to southern most sites in all values measured (Figure 8). Carbon content in stem and leaf tissue ranged between 45.7% and 57.9% and 45.2% and 48.5%, respectively (Appendix A). On average stems contain the highest amount of C% and N% of 50.0% and 46.7%, respectively.

A paired t-test was performed suggesting there is a significant difference between the carbon content measured in the stems and leaves ( $P=0.0008$ ). At all locations ( $n=13$ ) the difference in C% of the stems and leaves varied between  $-9.4$  and  $+0.9\%$  with a mean difference of  $-3.3\%$ . Changes in carbon content were correlated between the stems and leaves ( $r^2=0.32$ ) suggesting that an increase in carbon content of stems corresponds with an increase in carbon content of leaves.

The mean difference in N% of stems and leaves at all locations was  $-0.23\%$  and ranged between  $-0.52$  and  $+0.01\%$ . The paired t-test suggested there is a significant difference between the nitrogen content in the leaves compared to the stems ( $P=0.0002$ ). The between-site differences in N% of the stem and leaf tissue was minimal varying between  $-0.52$  and  $+0.01\%$ . There was a positive correlation ( $r^2=0.53$ ) between stems and leaf N% suggesting an increase in N% in stems corresponds with an increase in N% in leaves.

The average C:N ratios for stems and leaves was 43.3 and 55.2, respectively, with stem C:N ratios ranging from 26.0 to 58.1 and leaf ratios ranging from 32.8 and 90.8. The

relatively low average N% in leaves resulted in higher C:N ratios compared to that of stems (Appendix A).

### 3.1.2 $\delta^{13}\text{C}$ VALUES

The  $\delta^{13}\text{C}$  values showed a semi consistent offset between the two tissue types, with stems displaying more depleted values than the leaves (Figure 8). The range in  $\delta^{13}\text{C}$  values in stems was from  $-28.1$  to  $-32.0\text{‰}$  with the sample from Hermit Island ( $64^{\circ}48'S$ ) having the most depleted value of  $-32.0\text{‰}$ . The range in  $\delta^{13}\text{C}$  values of modern *P. strictum* leaves were consistently more enriched than stems with values ranging from  $-27.0$  to  $-29.7\text{‰}$ . The mean difference between  $\delta^{13}\text{C}$  values of the leaves and stems was  $2.0\text{‰}$  and ranged between  $+0.6$  and  $+3.1\text{‰}$ . The paired t-test suggested there is a significant difference between the  $\delta^{13}\text{C}$  values of stems and leaves ( $P \ll 0.05$ ).

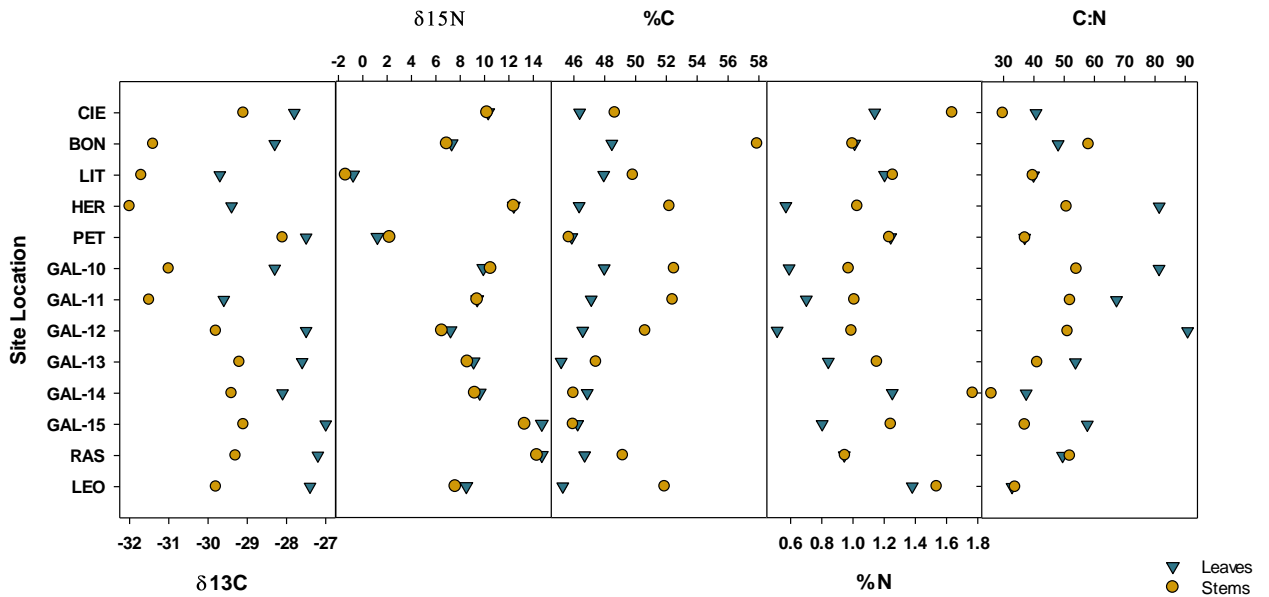


**Figure 8.** Values of isotopes of carbon ( $\delta^{13}\text{C}$ ) and nitrogen ( $\delta^{15}\text{N}$ ), carbon content (C%), nitrogen content (N%), and C:N ratio for *Polytrichum strictum* stems and leaves that were collected from 13 populations at 7 sites along the western AP.

### 3.1.3 $\delta^{15}\text{N}$ VALUES

The  $\delta^{15}\text{N}$  values of modern plant tissues showed more variation between sites than between plant tissue. The mean difference between  $\delta^{15}\text{N}$  values of leaves and stems was 0.29‰ and ranged between  $-1.0$  and  $+1.4$ ‰. It is evident by the  $\delta^{15}\text{N}$  values that there is less tissue effect and the difference in tissue  $\delta^{15}\text{N}$  values is more influenced by geographic location. There is a small difference between  $\delta^{15}\text{N}$  values in stems and leaves ( $P=0.06$ ) after running a paired t-test. There is a strong positive correlation between the  $\delta^{15}\text{N}$  values of stems and leaves ( $r^2=0.98$ ) suggesting the  $\delta^{15}\text{N}$  values of stems and leaves are relatively the same at all locations.

### 3.2 GALINDEZ ISLAND BULK SEDIMENT CORE

Bulk sediment from the Galindez island core was measured for its  $\delta^{13}\text{C}$ , bulk density, and total C (TC%), total N (TN%), and OM content (Figure 9). TN% and TC% is used in the measurement of bulk sediment representing the percentage of total N and C content in the sediment. There is a large shift towards a positively increasing bulk density starting at around 30 cm possibly due to a shift in snow or ice cover or shift in plant composition. TN% shows highly variable results throughout the entire length of the core. In contrast, very little variation is observed in the TC% throughout most of the length of the core. The C:N ratios measured in the top five centimeters revealed the highest values between  $+33.3$  to  $+72.8$  suggesting N was limited during that time. The bulk  $\delta^{13}\text{C}$  values exhibit the most depleted values seen throughout any other time period in the core between  $-24.8$  and  $-27.6$ ‰.

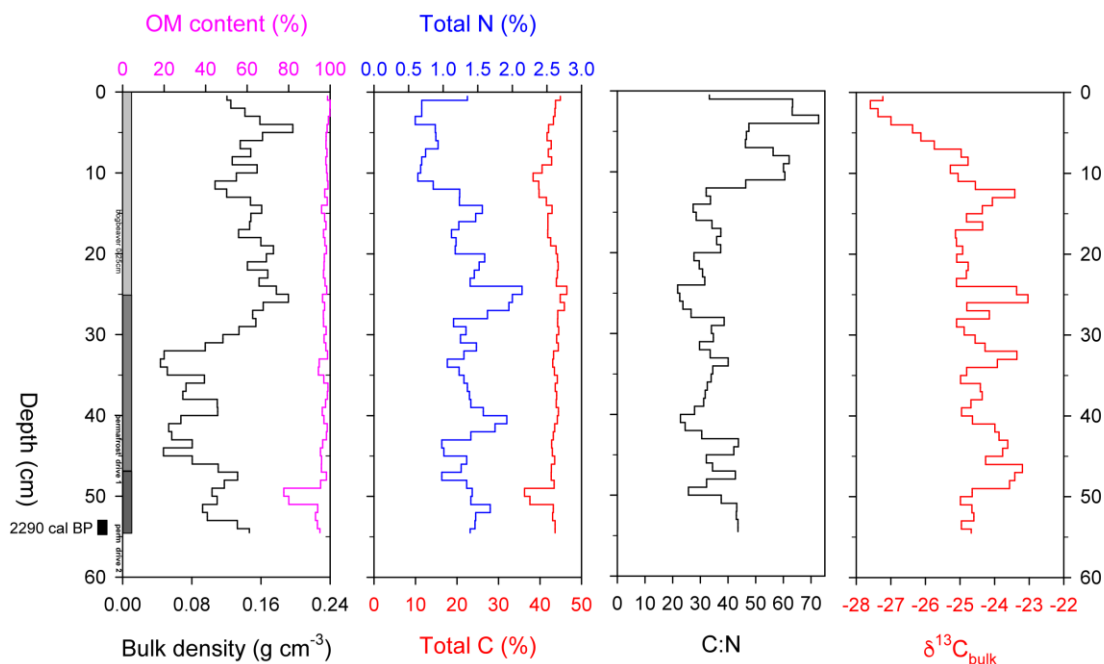


**Figure 9.** Galindez Island bulk sediment core profile illustrating the values of organic matter content (OM%), bulk density, total carbon and nitrogen, C:N ratios, and bulk carbon isotope values ( $\delta^{13}\text{C}_{\text{bulk}}$ ) for every centimeter in the core.

### 3.3 GALINDEZ ISLAND FOSSIL LEAF MATERIAL

#### 3.3.1 ACIDIFIED VS. NON-ACIDIFIED TEST

To eliminate the chance of fractionation errors from carbonates in our stable carbon isotope analysis, a comparison was made using *P. strictum* leaves from five levels. A paired t-test was performed to see if acidification was necessary. The acidified ( $n=5$ ) and non-acidified ( $n=5$ ) means of the carbon content were plotted with their standard error ( $37.5 \pm 2.4\%$  and  $37.0 \pm 2.0\%$ , respectively) and acidifying the leaves showed no significant influence on carbon content ( $P=0.1619$ ) (Figure 10a). The means of  $\delta^{13}\text{C}$  values for acidified ( $n=5$ ) and non-acidified ( $n=5$ ) leaves were also plotted with their standard error ( $-24.9 \pm 0.38\text{‰}$  and  $-24.7 \pm 0.34\text{‰}$ , respectively) and acidifying the leaves had no significant influence on the  $\delta^{13}\text{C}$  values ( $P=0.1177$ , Figure 10b).

Minimal differences were also seen in acidified and non-acidified samples of N% and  $\delta^{15}\text{N}$  values (Figure 10c, 10d). Despite the non-acidified leaves having no significance on the carbon content and  $\delta^{13}\text{C}$  values, it was decided to acidify all leaves prior to further analysis.

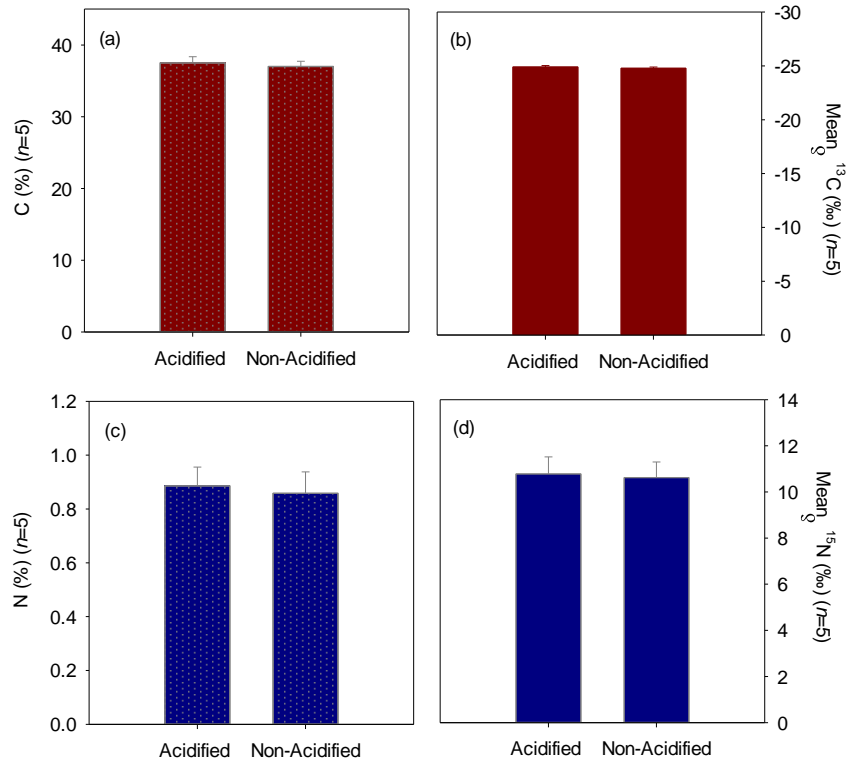


**Figure 10.** a) Mean values and standard error plotted for **a)** acidified ( $37.5 \pm 0.87\%$ ) and non-acidified ( $37.0 \pm 0.73\%$ ) C%, **b)** acidified ( $-24.9 \pm 0.14\text{‰}$ ) and non-acidified ( $-24.7 \pm 0.12\text{‰}$ )  $\delta^{13}\text{C}$  values, **c)** acidified ( $0.89 \pm 0.07\%$ ) and non-acidified ( $0.85 \pm 0.08\%$ ) N%, and **d)** acidified ( $10.8 \pm 0.74\text{‰}$ ) and non-acidified ( $10.6 \pm 0.68\text{‰}$ )  $\delta^{15}\text{N}$  values.

### 3.3.2 $\delta^{13}\text{C}$ VALUES

The  $\delta^{13}\text{C}$  values of fossil *P. strictum* leaves from each interval of the core showed limited variation of 2.6‰ from the base of the core to 10 cm depth, with values ranging between  $-23.7$  to  $-26.3\text{‰}$ . At 10 cm the trend shifts towards increasing depleted values



between  $-25.3$  to  $-30.3\text{‰}$  (Figure 11a).

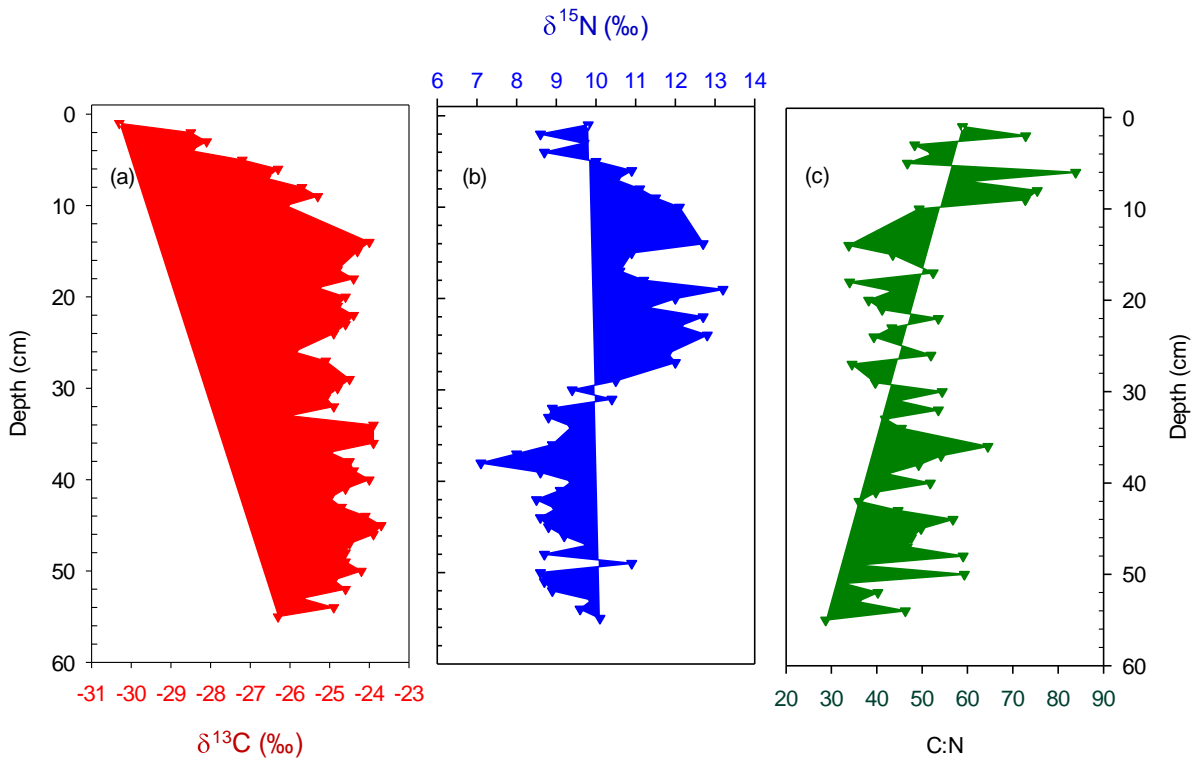


**Figure 11.** Values of a) isotopes of carbon ( $\delta^{13}\text{C}$ ) and b) nitrogen ( $\delta^{15}\text{N}$ ) and c) C:N ratios measured using *P. strictum* leaves found within the Galindez Island core.

### 3.3.3 $\delta^{15}\text{N}$ VALUES

The  $\delta^{15}\text{N}$  values measured showed high variability throughout the length of the core (Figure 11b). Most depleted values were measured between 37 and 39 cm ranging between  $+7.0$  and  $+8.7\text{‰}$  with an increasing trend towards more enriched values deposited immediately after. The most enriched trend compared to any other depth was deposited between 8 and 23 cm with  $\delta^{15}\text{N}$  values ranging from  $+10.0$  to  $+13.2\text{‰}$ . Most recent deposits starting at 5 cm depth shift towards more depleted  $\delta^{15}\text{N}$  values ranging from  $+8.6$  to  $+9.8\text{‰}$ .

### 3.4 RADIOCARBON AGE ESTIMATES

Measurement of radiocarbon content using bulk peat at the base of the Galindez island core shows the peat bank ecosystem is roughly 2290 years old, making it one of the oldest cores ever retrieved from the Antarctic Peninsula. Ages of *P. strictum* leaves and stems ranged from  $295 \pm 30$  and  $2290 \pm 150$  cal year BP and showed no reversed dates in the profile (Table 1).

#### 3.4.1 AGE-DEPTH MODEL

An age-depth model was constructed from the iterative program, BACON, using Bayesian statistics to reconstruct Bayesian accumulation deposits (Blaauw & Christen 2005). The age-depth model was determined using thousands of Markov Chain Monte Carlo (MCMC) iterations understanding that all radiocarbon determinations incorporate the uncertainty in the calibrated calendar range from the  $2\sigma$  range of radiocarbon determinations. Radiocarbon dates obtained from the six levels throughout the core were plotted as an age-depth model (Figure 12). The age-depth model suggests a possible hiatus between 700 and 1450 cal yr BP (Figure 12a). Little to no accumulation occurred for about 700 years during this time suggesting there may have been a period significant snow or ice cover that stopped plant growth. Sedimentation rates (Figure 12b) show accumulation begins promptly after the hiatus.

**Table 1.**  $^{14}\text{C}$ -AMS Measurements of *Polytrichum* Leaf Fossil Age at Four Intervals of GAL-3 Core and One Bulk Peat, Listed by Decreasing Depth

Site	Dated Depth (cm)	Lab #	Material Dated	$\delta^{13}\text{C}$ (‰ PDB)	$^{14}\text{C}$ (years BP)	Median Age (calendar years BP)	$2\sigma$ Age Range (calendar years BP)
GAL 3	13-14	CAMS-173288	<i>Polytrichum</i> leaves	-25	295±30	313	154-445
GAL 3	21-22	CAMS-173289	<i>Polytrichum</i> leaves	-25	410±30	445	325-499
GAL 3	28-29	CAMS-173290	<i>Polytrichum</i> leaves	-25	1449±30	1392	1315-1505
GAL 3	44-45	CAMS-173291	<i>Polytrichum</i> leaves	-25	1855±30	1748	1623-1828
GAL 3	52-54	CAMS-170242	Moss stems	-25	2290±150	2260	1929-2711

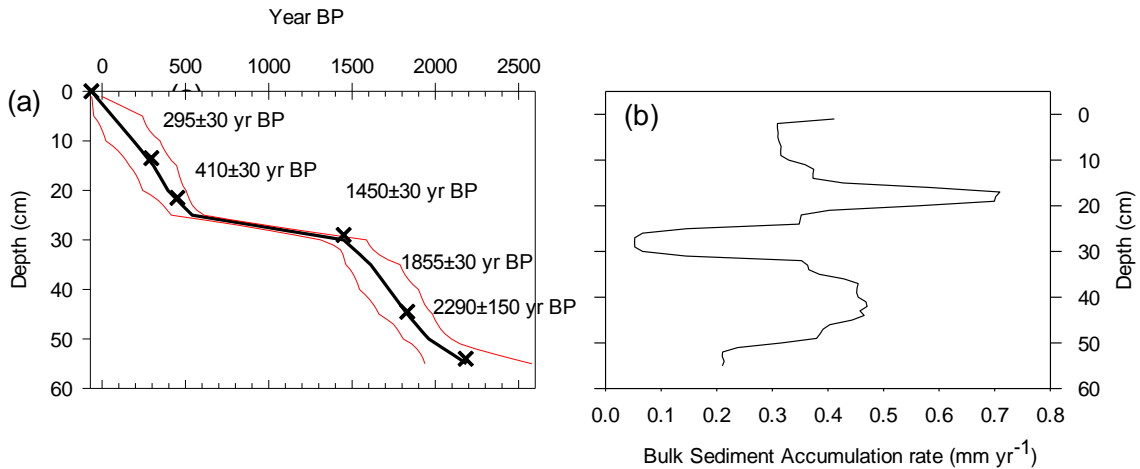


**Figure 12.** a) Radiocarbon age-depth curve for the Galindez Island peat core. Measured ages were calibrated using CALIB 7.0.4. b) Sediment accumulation rates calculated using the sediment bulk density values of the Galindez Island core and the calibrated radiocarbon ages.

### 3.4.2 C, OM, DRY MASS ACCUMULATION RATES

The accumulation rates for C, OM, and dry mass (Figure 13) show the same hiatus in the age-depth model and sedimentation accumulation rates observed from Figure 11. A large peak in dry mass, C, and OM accumulation rates occurs at 400 cal yr BP with max values of 111.7, 47.5, and 108.9 g m<sup>-2</sup> yr<sup>-1</sup>, respectively. Carbon accumulation rates before the hiatus were as low as 3.5 g m<sup>-2</sup> yr<sup>-1</sup> with values never reaching as low after the hiatus. Similarly, OM and dry mass accumulation rates reached values as low as 7.6 and 7.8 g m<sup>-2</sup> yr<sup>-1</sup>, respectively before the start of the hiatus.

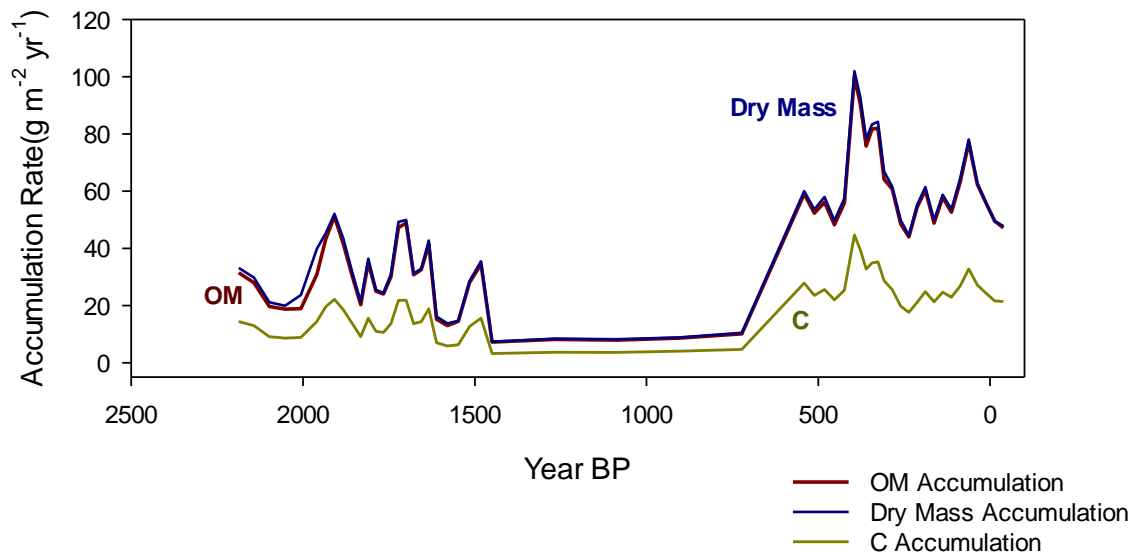


**Figure 13.** Accumulation rates measured in  $\text{g m}^{-2} \text{yr}^{-1}$  for dry mass (blue), carbon (C) (yellow), and organic matter (OM) (dark red).

## 4.0 DISCUSSION

### 4.1 MODERN TISSUE STABLE CARBON AND NITROGEN VARIATION

The effect of recent warming on *P. strictum* mosses along the AP was complex. Previous studies have observed *Polytrichum* moss species as isolated plants in Arctic polar regions growing amongst dominating *Sphagnum* species (Bu et al., 2011). However, on the AP modern *P. strictum* mosses dominate regions by forming large dense patches, which is most likely the result of being one of the first moss species to colonize this area (Fenton & Smith 1982). It is suggested by the variation in the results of our stable isotope values that the response of *P. strictum* plants under recent warming is influenced by factors other than air temperature, such as changes in the amount of solar radiation intensity and its effect on surface temperature, water and nutrient availability, or biomolecular differences of plant tissue (Bu et al., 2011; Royles et al., 2014).

The control on what was causing the significantly more depleted  $\delta^{13}\text{C}$  values of stems compared to the leaves was unclear from the data plotted in Figure 8. To better understand what is driving the differences in stem and leaf  $\delta^{13}\text{C}$  values, I compared each tissue's  $\delta^{13}\text{C}$  values to their C:N ratios (Figure 14). There was a significant ( $P < 0.001$ ) and negative correlation ( $r^2 = 0.34$ ) between stem  $\delta^{13}\text{C}$  values and stem C:N values, indicating that when stems exhibit enriched  $\delta^{13}\text{C}$  values the C:N ratio will be low, or vice versa when stems exhibit depleted  $\delta^{13}\text{C}$  values, stem C:N ratios will be high. This negative correlation suggests higher C:N ratios are driven by low N content when discrimination is high. The ombrotrophic environment associated with the *P. strictum* plant populations in this study indicates these plants are dependent on atmospheric deposition for N inputs. Typically, drier conditions would result in low N availability and limited discrimination

due to heightened plant stress, however the relationship between stem  $\delta^{13}\text{C}$  values and their C:N ratios suggests this is not the case. Instead, the data represented in Figure 13 suggest drier *P. strictum* mosses discriminate more against  $^{13}\text{C}$ . The lack of correlation between the  $\delta^{13}\text{C}$  values and C:N ratios of leaves might suggest leaf tissue responses are controlled by local climate or weather conditions. The sensitivity of leaf tissue to local climate conditions is therefore important to consider when using *P. strictum* leaves to interpret paleoclimate conditions.

Royles *et al.* (2016) argued that when little biotic competition and strong physical environmental drivers exists, responses of biological systems are not directly related to broad-scale climate but instead strongly influenced by microclimate. Additionally, the physical changes (i.e. leaf folding over lamellae) *Polytrichum* plants undergo to avoid water stress can alter the effectiveness of  $\text{CO}_2$ -uptake in the plant by creating a larger diffusional barrier (Thomas *et al.*, 1996).

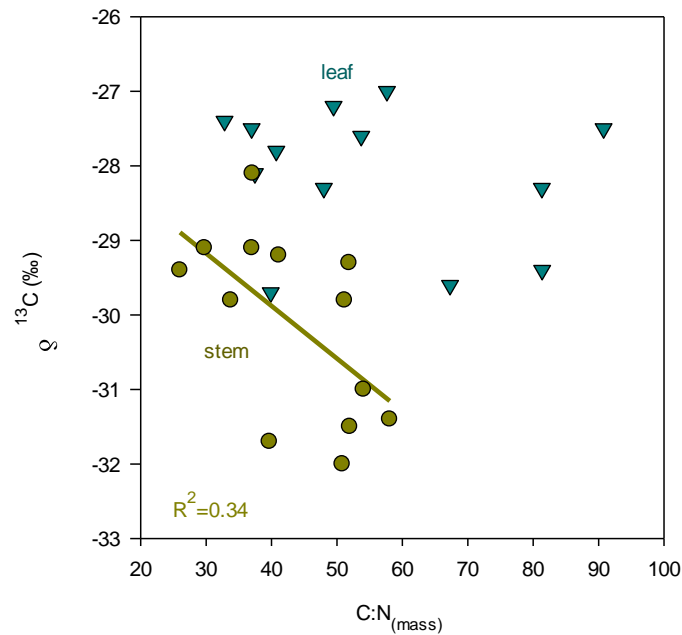


**Figure 14.** Stem (yellow circles) and leaf (teal triangles) C:N ratios plotted against their  $\delta^{13}\text{C}$  values. Stems have a negative correlation ( $R^2=0.34$ ) indicated by the regression line.

The range in  $\delta^{15}\text{N}$  values observed from modern plant tissue suggests variation in N inputs in each population. The slightly negative  $\delta^{15}\text{N}$  value of the Litchfield Island plant sample may reflect an isotopically depleted ammonia source which indicates the N source was derived from either penguins or atmospheric  $\text{NH}_3$  (Lee et al., 2009; Huiskes et al., 2006). The more enriched values of  $\delta^{15}\text{N}$ , with values ranging between +6.0 and +15.0‰, are likely from N inputs coming from seabird or seal excrement.

#### **4.2 AGE-DEPTH MODEL HIATUS AND ACCUMULATION RATES**

The radiocarbon age estimated at the base of the Galindez Island core suggests accumulation of this moss bank began around 2290 cal yr BP. There is evidence of a hiatus that began around 1450 cal yr BP that can possibly be explained by a cold period lasting between 1450 and 700 cal yr BP. Sea ice growth started around 1500 cal yr BP in Barilari Bay following its retreat around 80 cal yr BP according to Christ et al. (2015, Figure 5a).

In the peat core, the average accumulation rate of OM from 2290 to 1450 cal yr BP (before the start of the hiatus) was  $\sim 28.8 \text{ g m}^{-2} \text{ yr}^{-1}$ , which was less than the average accumulation rate of OM after the hiatus starting at 750 cal yr BP of  $\sim 56.2 \text{ g m}^{-2} \text{ yr}^{-1}$ . This difference, however, may be due to the decomposition of organic matter at lower depths even at slow rates. If productivity at the surface remained constant, it is expected that decay below the surface would follow with depth (Clymo 1984). Decreases in apparent accumulation rates observed between 700 and 100 years BP (Figure 13) therefore represent periods associated with a change in productivity that caused accumulation and decomposition to slow down. Furthermore, accumulation rates of OM or C observed at deeper depths (older) of the core have more time to decompose than the



accumulation rates observed at shallower depths, so accumulation rates would generally be higher at the top of the core profile (Clymo 1984) as seen in the trends of accumulation rates of the Galindez Island core in Figure 13.

A peak in C, OM, and dry mass accumulation rates is observed around 400 years BP, suggesting the rate of plant growth around that time was highest compared to any other peak observed throughout the core. Following the highest peak, was the largest decrease in rates seen between 300 and 200 years BP. Overall, there was more variability in accumulation rates observed after the hiatus compared to variability observed before the hiatus.

#### **4.3 FOSSIL LEAF STABLE ISOTOPE VARIATION**

The stable C and N isotope values of fossil leaves from the Galindez Island core revealed many variations over the last 2290 years. There was a small variation (2.6‰) observed in the  $\delta^{13}\text{C}$  values from 200 cal year BP to the base of the core (2290 cal year BP) (Figure 15a). However, trends observed from the source independent discrimination (Figure 16a) derived from the  $\delta^{13}\text{C}$  values in Figure 15a showed more pronounced variability in discrimination over the last 2290 years.

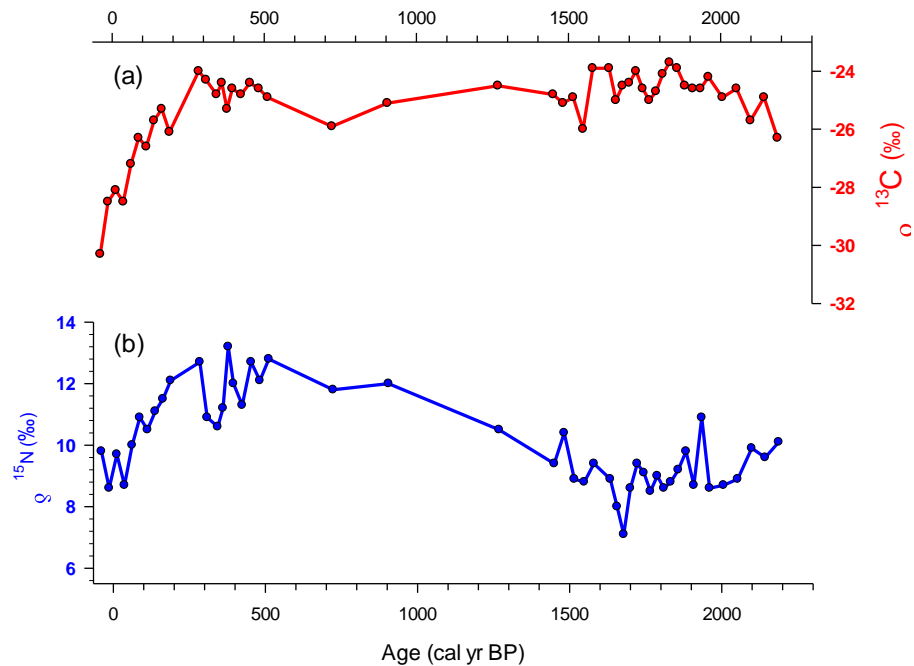


**Figure 15.** Galindez island core fossil leaf stable isotope values over the last 2290 years **a)** Plot of stable carbon isotope values of fossil leaves over time. **b)** Stable N isotope values of fossil leaves over time.

A relatively high discrimination at the base of the core suggested conditions at that time were suitable for plant growth. Discrimination gradually decreased between 1900 to 1500 years BP around the time of the onset of the icy cold period (Figure 16b). The lowest discrimination was observed between 1500 and 1100 years BP followed by a brief increase in discrimination at around 950 years BP, which was associated with cooler SST's (Figure 16c). The discrimination from 1500 and 1100 years BP was similar to the one observed at the base of the core suggesting temperatures at the time promoted ice melt to allow plants to grow for a short time. A shift towards increasing bulk density at 30 cm (~1000 years BP) seen in Figure 9 occurred roughly around the start of the hiatus providing some evidence to support increase in snow or ice extent during the time discrimination was lowest.

Immediately after the brief increase in discrimination and the suggested hiatus in the age-depth model (Figure 12a), discrimination decreases again until around 500 years BP. At 500 years BP there was an increase in discrimination that is similar to the small peak observed around 950 years BP that was associated with cooler SST's (Figure 16c), suggesting more favorable climate conditions allowed plants to grow for a short time before switching again towards lower discrimination values. The highest discrimination made by *P. strictum* plants over the last 2290 years, independent of the recent depletion in atmospheric  $\delta^{13}\text{C}$ , was observed over the last two centuries. Sediment cores, analyzed by Christ et al. (2014), suggested there was an increase in glacial melt that occurred around the time the highest discrimination is observed and when SST's were cooler (Figure 16). This suggests that the increase in discrimination made by *P. strictum* in most recent decades is associated with an increase in glacial melt and colder SST's. It is evident that higher discrimination seems to reflect periods of colder SST's when comparing source independent discrimination to Palmer Deep SST's of the same time period (Figure 16a, 16c).

Variability in  $\delta^{15}\text{N}$  values throughout the depth of the core suggests nitrogen sources and amounts have varied over time (Figure 15b). Variation in N sources and amounts is supported by the fact that this peat bank is ombrotrophic implying N is limited in this ecosystem and therefore any N that becomes available to plants will be taken up (Asada et al., 2005). Specifically, between 700 and 200 years BP when enriched  $\delta^{15}\text{N}$  values of +11.5 to +13.2‰ in leaf tissue were measured, there may have been trophically-enriched inputs of N from seabirds. The enriched  $\delta^{15}\text{N}$  values associated with seabird excrement was likely derived by melt water given that  $\delta^{15}\text{N}$  values are most

enriched was right after the hiatus, indicating ice or snow melt occurred thus putting more N into the soils (Huiskes et al., 2006).

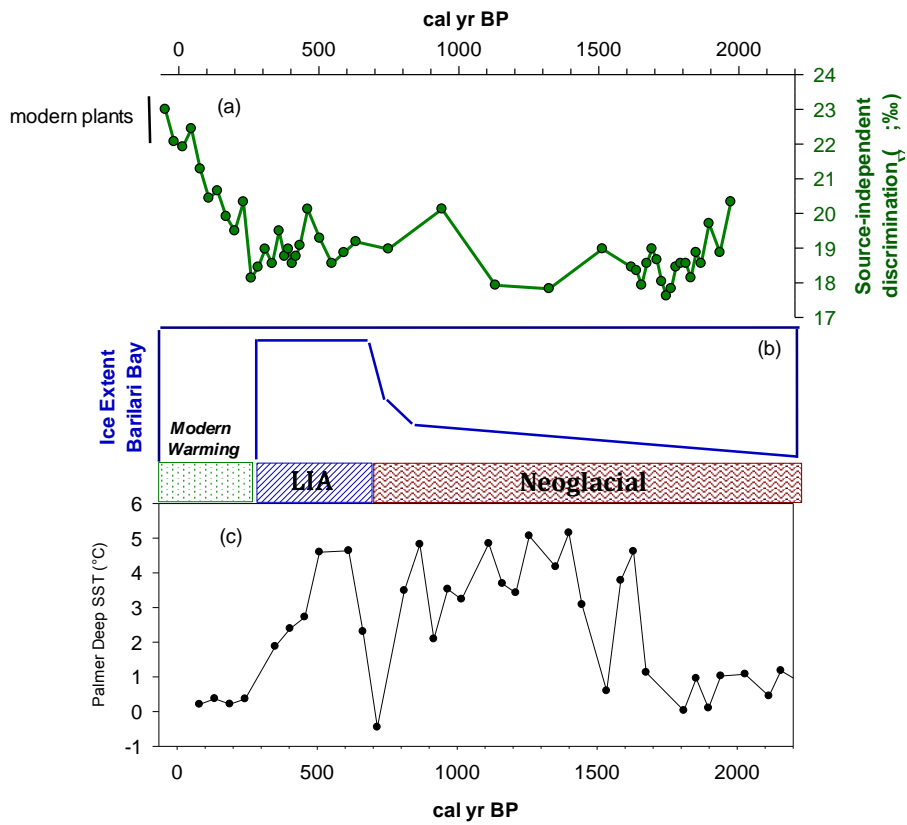


**Figure 16.** (left) **a)** Source-independent discrimination of  $^{13}\text{C}$  made by *P. strictum* plants. **b)** Approximation of Barilari Bay sea ice extent over the last 2300 years based on sediment core data from Christ et al. (2014). **c)** Palmer Deep sea surface temperature (SST) observed over the last 2300 years (Shevenell et al., 2011).

## 5.0 CONCLUSION AND FUTURE DIRECTIONS

The discrimination against  $^{13}\text{C}$  measured in the tissue of *P. strictum* plants was more complex than expected. Stable carbon isotope values that were compared to the C:N ratios of modern plant leaves provided some evidence to support *P. strictum* leaf tissue content displays more sensitivity to local climate variations rather than reflecting the internal allocation of nutrients within the tissue. Future research will compare the stable C and N values of tissue from *P. strictum* mosses to another dominating moss species collected from similar sites along the AP to assess the drivers of  $^{13}\text{C}$  values within and between peatbank species to better understand their sensitivity and resilience to climate change over time.

*P. strictum* fossil leaves were present throughout the 2290 year old core, providing evidence to support that this was one of the first moss species to colonize the AP and that they have thrived at the location since. This moss is dominant in the region where it forms large banks that have only been observed to occur on the AP. The introduction of new moss species may threaten *P. strictum* populations, as other moss species, such as *Sphagnum* mosses, have been found to outcompete *Polytrichum* mosses. The limited variation in stable carbon isotopes over time from 2290 years BP until around 200 years BP suggests no significant climate event was able to permanently shut down the production of *P. strictum* plants. Evidence of sea ice extent around the same time as the suggested hiatus in the age-depth model suggests the hiatus may have been caused by ice advancing and remaining on the moss bank surface for about 700 years prior to it melting and the restarting of rapid accumulation around 400 years ago.

Discrimination made by *P. strictum* plants in most recent decades showed the highest values observed in the last 2290 years indicating there were no significant climate events in the last two centuries that caused discrimination by *P. strictum* plants to decrease. There was evidence that supported higher discrimination may reflect times of cooler SST's, and warmer SST's were roughly around the times when discrimination was lowest (Christ et al., 2014; Shevenell et al., 2011). To provide a more accurate age-depth chronology to support the timing of this recent discrimination, more radiocarbon dates will need to be determined from the upper 20 cm of the Galindez Island core. A cellulose extraction on the fossil leaves is another step to take to compare the  $\delta^{13}\text{C}$  values from the cellulose to the  $\delta^{13}\text{C}$  values from the bulk leaves to provide stronger evidence to support the variation that was observed throughout the core. Additionally, a macrofossil analysis will be performed to reconstruct the vegetation on Galindez Island over the last 2300 years would provide insight to possible controls on  $\delta^{13}\text{C}$  values in *P. strictum* plants leaves.

APPENDIX A: Modern Leaf-Stem Results and Site Locations

Sample Name	Site Location	Latitude (South)	Longitude (West)	$\delta^{15}\text{N}$ (‰)	$\delta^{13}\text{C}$ (‰)	N Content (%)	C Content (%)	C:N
ANT14_CIE_13L	Cierva	64° 09' 20.00"	60° 57' 22.00"	10.3	-27.8	1.14	46.37	40.7
ANT14_CIE_13S	Cierva	64° 09' 20.00"	60° 57' 22.00"	10.2	-29.1	1.64	48.65	29.7
ANT14_BON_02L	Bonaparte	64° 46' 34.85"	64° 03' 08.00"	7.3	-28.3	1.01	48.46	48.0
ANT14_BON_02S	Bonaparte	64° 46' 34.85"	64° 03' 08.00"	6.9	-31.4	1.00	57.89	58.1
ANT14_LIT_04L	Litchfield	64° 46' 12.90"	64° 05' 20.10"	-0.8	-29.7	1.20	47.93	39.9
ANT14_LIT_04S	Litchfield	64° 46' 12.90"	64° 05' 20.10"	-1.4	-31.7	1.26	49.82	39.7
ANT14_HER_04L	Hermit	64° 48' 00.00"	64° 01' 04.00"	12.4	-29.4	0.57	46.34	81.4
ANT14_HER_04S	Hermit	64° 48' 00.00"	64° 01' 04.00"	12.4	-32.0	1.03	52.20	50.8
ANT14_PET_02L	Petermann	64° 10' 20.00"	64° 08' 18.00"	1.2	-27.5	1.24	45.86	37.0
ANT14_PET_02S	Petermann	64° 10' 20.00"	64° 08' 18.00"	2.2	-28.1	1.23	45.68	81.3
ANT14_GAL_10L	Galindez	65° 14' 51.40"	64° 15' 02.30"	9.9	-28.3	0.59	47.96	54.0
ANT14_GAL_10S	Galindez	65° 14' 51.40"	64° 15' 02.30"	10.5	-31.0	0.97	52.50	67.3
ANT14_GAL_11L	Galindez	65° 14' 51.40"	64° 15' 02.30"	9.4	-29.6	0.70	47.13	52.0
ANT14_GAL_11S	Galindez	65° 14' 51.40"	64° 15' 02.30"	9.4	-31.5	1.01	52.40	90.8
ANT14_GAL_12L	Galindez	65° 14' 51.40"	64° 15' 02.30"	7.2	-27.5	0.51	46.57	51.1
ANT14_GAL_12S	Galindez	65° 14' 51.40"	64° 15' 02.30"	6.5	-29.8	0.99	50.62	53.7
ANT14_GAL_13L	Galindez	65° 14' 51.40"	64° 15' 02.30"	9.1	-27.6	0.84	45.78	41.1
ANT14_GAL_13S	Galindez	65° 14' 51.40"	64° 15' 02.30"	8.6	-29.2	1.15	47.43	37.4
ANT14_GAL_14L	Galindez	65° 14' 51.40"	64° 15' 02.30"	9.6	-28.1	1.25	46.86	26.0
ANT14_GAL_14S	Galindez	65° 14' 51.40"	64° 15' 02.30"	9.2	-29.4	1.77	45.97	57.6
ANT14_GAL_15L	Galindez	65° 14' 51.40"	64° 15' 02.30"	14.7	-27.0	0.80	46.24	37.0
ANT14_GAL_15S	Galindez	65° 14' 51.40"	64° 15' 02.30"	13.3	-29.1	1.24	45.94	49.5
ANT14_RAS_05L	Rasmussen	65° 14' 49.50"	64° 65' 06.80"	14.7	-27.2	0.94	46.69	49.5
ANT14_RAS_05S	Rasmussen	65° 14' 49.50"	64° 65' 06.80"	14.3	-29.3	0.95	49.17	51.9
ANT14_LEO_07L	Leonie	67° 35' 55.00"	68° 21' 21.00"	8.5	-27.4	1.38	45.28	32.8
ANT14_LEO_07S	Leonie	67° 35' 55.00"	68° 21' 21.00"	7.6	-29.8	1.54	51.89	33.8

Appendix B: GAL-3 Bulk Sediment Results

Depth (cm)	BD (g/cm <sup>3</sup> )	OM %	C%	N%	C:N	δ <sup>13</sup> C
1	0.1205	98.70	44.88	1.35	33.3	-27.2
2	0.1250	100.00	43.72	0.69	63.4	-27.6
3	0.1414	99.86	43.57	0.69	63.2	-27.4
4	0.1586	99.11	43.22	0.59	72.8	-27.0
5	0.1968	98.49	42.04	0.88	47.6	-26.4
6	0.1617	98.03	41.67	0.89	46.7	-26.1
7	0.1360	97.97	42.68	0.92	46.3	-25.7
8	0.1481	98.41	42.00	0.75	56.3	-25.0
9	0.1266	97.91	42.79	0.69	62.1	-24.8
10	0.1555	98.27	40.49	0.67	60.1	-25.3
11	0.1314	98.54	38.30	0.63	60.6	-25.1
12	0.1068	98.93	39.70	0.85	46.4	-24.6
13	0.1203	97.35	39.73	1.24	32.1	-23.4
14	0.1478	98.55	41.53	1.23	33.7	-24.1
15	0.1606	95.82	42.88	1.56	27.4	-24.4
16	0.1483	97.32	41.87	1.47	28.5	-24.8
17	0.1468	98.00	41.89	1.22	34.2	-24.3
18	0.1340	96.77	41.85	1.12	37.4	-25.1
19	0.1598	97.42	42.55	1.18	35.9	-25.1
20	0.1743	98.15	43.86	1.17	37.4	-24.9
21	0.1662	97.19	44.20	1.60	27.7	-25.1
22	0.1442	97.05	44.34	1.52	29.6	-24.8
23	0.1678	96.77	44.15	1.45	30.8	-24.8
24	0.1577	97.53	43.93	1.39	31.6	-25.1
25	0.1777	98.31	46.46	2.14	21.8	-23.4
26	0.1915	96.31	44.85	2.00	22.6	-23.0
27	0.1624	97.30	45.86	1.95	23.7	-24.8
28	0.1503	96.73	44.25	1.64	26.7	-24.2
29	0.1540	96.77	44.21	1.15	38.6	-25.1
30	0.1345	98.03	44.49	1.33	34.0	-24.9
31	0.1159	97.05	44.00	1.25	34.7	-24.6
32	0.0955	97.90	44.37	1.48	29.7	-24.3
33	0.0479	98.70	43.25	1.30	33.6	-23.4
34	0.0436	94.68	43.05	1.06	40.1	-23.9
35	0.0516	94.31	43.45	1.23	34.5	-24.8
36	0.0945	96.88	44.15	1.30	33.9	-25.0



<b>37</b>	0.0732	98.90	43.66	1.35	32.5	-24.4
<b>38</b>	0.0696	98.64	43.99	1.38	31.8	-24.4
<b>39</b>	0.1094	97.74	43.87	1.40	31.2	-24.7
<b>40</b>	0.1098	96.18	44.41	1.58	27.9	-25.0
<b>41</b>	0.0673	96.99	44.16	1.92	22.8	-24.6
<b>42</b>	0.0533	98.60	43.51	1.75	24.5	-24.0
<b>43</b>	0.0567	98.17	43.19	1.40	30.5	-23.9
<b>44</b>	0.0804	96.36	42.78	0.98	43.8	-23.6
<b>45</b>	0.0472	95.29	42.95	1.01	42.1	-23.8
<b>46</b>	0.0804	95.80	43.53	1.34	32.2	-24.3
<b>47</b>	0.1105	95.76	42.70	1.26	34.4	-23.2
<b>48</b>	0.1329	98.18	42.69	0.98	42.7	-23.4
<b>49</b>	0.1175	95.35	43.39	1.34	32.3	-23.6
<b>50</b>	0.1032	77.60	36.26	1.42	25.7	-24.6
<b>51</b>	0.1093	80.03	37.56	1.40	37.6	-25.0
<b>52</b>	0.0924	93.98	43.19	1.68	43.2	-24.7
<b>53</b>	0.0979	92.93	43.03	1.47	43.0	-24.6
<b>54</b>	0.1326	93.82	43.62	1.46	43.6	-25.0
<b>55</b>	0.1464	95.04	43.62	1.39	43.6	-24.7

Appendix C: GAL-3 Fossil Leaf Results

<b>Depth (cm)</b>	<b>mg N</b>	<b>mg C</b>	<b>%N</b>	$\delta^{15}\text{N}$	<b>%C</b>	$\delta^{13}\text{C}$	<b>C:N</b>
<b>1</b>	0.02	1.14	0.76	9.8	44.48	-30.3	58.91
<b>2</b>	0.01	1.09	0.60	8.6	43.39	-28.5	72.83
<b>3</b>	0.02	1.09	0.89	9.7	43.08	-28.1	48.37
<b>4</b>	0.02	1.11	0.83	8.7	43.45	-28.5	52.41
<b>5</b>	0.02	1.09	0.92	10.0	43.00	-27.2	46.74
<b>6</b>	0.01	1.07	0.51	10.9	42.85	-26.3	83.86
<b>7</b>	0.02	1.08	0.72	10.5	42.97	-26.6	60.06
<b>8</b>	0.01	1.08	0.57	11.1	42.63	-25.7	75.38
<b>9</b>	0.01	1.06	0.58	11.5	42.06	-25.3	72.77
<b>10</b>	0.02	1.06	0.85	12.1	42.04	-26.1	49.35
<b>14</b>	0.03	1.11	1.31	12.7	44.32	-24.0	33.84
<b>15</b>	0.03	1.10	1.00	10.9	43.36	-24.3	43.53
<b>17</b>	0.02	1.10	0.83	10.6	43.29	-24.8	52.42
<b>18</b>	0.03	1.09	1.27	11.2	43.20	-24.4	34.03
<b>19</b>	0.02	1.08	0.98	13.2	42.85	-25.3	43.54
<b>20</b>	0.03	1.07	1.12	12.0	42.96	-24.6	38.23
<b>21</b>	0.03	1.09	1.05	11.3	43.13	-24.8	41.20
<b>22</b>	0.02	1.08	0.80	12.7	43.02	-24.4	53.59
<b>23</b>	0.03	1.08	0.98	12.1	42.65	-24.6	43.32
<b>24</b>	0.03	1.09	1.10	12.8	43.37	-24.9	39.36
<b>26</b>	0.02	1.10	0.82	11.8	42.82	-25.9	51.95
<b>27</b>	0.03	1.07	1.22	12.0	42.31	-25.1	34.55
<b>29</b>	0.03	1.10	1.10	10.5	43.71	-24.5	39.67
<b>30</b>	0.02	1.09	0.80	9.4	43.54	-24.8	54.41
<b>31</b>	0.02	1.09	0.97	10.4	43.35	-25.1	44.66
<b>32</b>	0.02	1.09	0.81	8.9	43.16	-24.9	53.58
<b>33</b>	0.03	1.11	1.05	8.8	43.89	-26.0	41.91
<b>34</b>	0.02	1.10	0.95	9.4	43.26	-23.9	45.44
<b>36</b>	0.02	1.09	0.66	8.9	42.77	-23.9	64.50
<b>37</b>	0.02	1.11	0.80	8.0	43.39	-25.0	54.19
<b>38</b>	0.02	1.09	0.88	7.1	43.20	-24.5	49.24
<b>39</b>	0.03	1.08	1.01	8.6	42.68	-24.4	42.18
<b>40</b>	0.02	1.08	0.82	9.4	42.45	-24.0	51.81
<b>41</b>	0.03	1.08	1.09	9.1	43.26	-24.6	39.81
<b>42</b>	0.03	1.09	1.21	8.5	43.51	-25.0	36.10
<b>43</b>	0.02	1.09	0.96	9.0	42.92	-24.7	44.70

<b>44</b>	0.02	1.08	0.76	8.6	42.92	-24.1	56.79
<b>45</b>	0.02	1.11	0.87	8.8	43.37	-23.7	49.77
<b>46</b>	0.02	1.10	0.91	9.2	43.44	-23.9	47.63
<b>47</b>	0.02	1.12	0.94	9.8	43.81	-24.5	46.72
<b>48</b>	0.02	1.10	0.74	8.7	43.50	-24.6	59.04
<b>49</b>	0.03	1.13	1.25	10.9	44.64	-24.6	35.64
<b>50</b>	0.02	1.11	0.74	8.6	43.96	-24.2	59.31
<b>51</b>	0.03	1.13	1.36	8.7	44.55	-24.9	32.66
<b>52</b>	0.03	1.13	1.09	8.9	44.04	-24.6	40.24
<b>53</b>	0.03	1.12	1.26	9.9	44.85	-25.7	35.68
<b>54</b>	0.02	1.11	0.96	9.6	44.43	-24.9	46.30
<b>55</b>	0.04	1.15	1.57	10.1	45.10	-26.3	28.73

## LITERATURE CITED

- Asada, T., Warner, B.G., Aravena, R. (2005). Nitrogen isotope signature variability in plant species from open peatland. *Aquatic Botany*, 82(4), 297-307.
- Barbara, L., Crosta, X., Leventer, A., Schmidt, S., Etourneau, J., Domack, E., Masse, G. (2015). Environmental responses of the northeast Antarctic Peninsula to the Holocene climate variability. *Paleoceanography*, 31, 131-147.
- Bentley, M.J., Hodgson, D.A., Smith, J.A., Cogaigh, C.O., Domack, E.W., Larter, R.D., Roberts, S.J., Brachfeld, S., Leventer, A., Hjort, C., Hillenbrand, C.D., Evans, J. (2009). Mechanisms of Holocene palaeoenvironmental change in the Antarctic Peninsula region. *The Holocene*, 19(1), 51-69.
- Beyer, L., and Bolter, M. (2002). *Geoecology of Antarctic Ice-Free Coastal Landscapes*. Springer, Heidelberg, Germany. 154, 51-65.
- Blaauw, M., and Christen, J.A. (2009). Flexible paleoclimate age-depth models using an autoregressive gamma process. *Bayesian Analysis*, 6(3), 457-474.
- Blaauw, M. (2010). Methods and code for 'classical' age-modelling of radiocarbon sequences. *Quaternary Geochronology*, 1-7.
- Bu, Z.J., Rydin, H., Chen, X. (2010). Direct and interaction-mediated effects of environmental changes on peatland bryophytes. *Oecologia*, 166, 555-563.
- Cannone, N., Binelli, G., Worland, M.R., Convey, P., Guglielmin, M. (2012). CO<sub>2</sub> fluxes among different vegetation types during the growing season in Marguerite Bay (Antarctic Peninsula). *Geoderma*, 189-190, 595-605.
- Charman, D. (2002). Peatlands and environmental change. *Land Degradation and Development*, 13(6), 527-528.
- Christ, A.J., Talaia-Murray, M., Elking, N., Domack, E.W., Leventer, A., Lavoie, C., Brachfeld, S., Yoo, K.C., Gilbert, R., Jeong, S.M., Petrushak, S., Wellner, J. (2014). Late Holocene glacial advance and ice shelf growth in Baralari Bay, Graham Land, west Antarctic Peninsula. *Geological Society of America*, 127(1/2), 297-315.
- Clymo, R.S. (1984). The limits to peat bog growth. *Philosophical Transactions of the Royal Society of London*, 303, 605-654.
- Clymo, R.S., Turunen, J., Tolonen, K. (1998). Carbon accumulation in peatlands. *Oikos*, 81, 368-388.

- Colwell, S. (2009). Palmer Station Temperature Data. [Annual temperatures between 1997 and 2014]. Retrieved from:  
<https://legacy.bas.ac.uk/met/READER/data.html>.
- Colwell, S. (2009). O'Higgins Station Temperature Data. [Annual temperatures between 1963 and 2015]. Retrieved from:  
<https://legacy.bas.ac.uk/met/READER/data.html>.
- Colwell, S. (2009). Rothera Station Temperature Data. [Annual temperatures between 1976 and 2015]. Retrieved from:  
<https://legacy.bas.ac.uk/met/READER/data.html>.
- Colwell, S. (2009). Vernadsky Station Temperature Data. [Annual temperatures between 1947 and 2015]. Retrieved from:  
<https://legacy.bas.ac.uk/met/READER/data.html>.
- Convey, P., Hopkins, D.W., Roberts, S.J., Tyler, A.N. (2011). Global southern limit of flowering plants and moss peat accumulation. *Polar Research*, 30, 1-10.
- Dawson, T.E., Mambelli, S., Plamboeck, A.H., Templer, P.H., Tu, K.P. (2002). Stable isotopes in plant ecology. *Annual Review of Ecology Systems*, 33, 507-559.
- Day, T.A., Ruhland, C.T., Xiong, F.S. (2008). Warming increases aboveground plant biomass and C stocks in vascular-plant-dominated Antarctic tundra. *Global Change Biology*, 14, 1827-1843.
- Etourneau, J., Collins, L.G., Willmott, V., Kim, J.-H., Barbara, L., Leventer, A., Schouten, S., Damste, J.S.S., Bianchini, A., Klein, V., Crosta, X., Masse, G. (2013). Holocene climate variations in the western Antarctic Peninsula: evidence for sea ice extent predominantly controlled by changes in insolation and ENSO variability. *Climate of the Past*, 9, 1431-1446.
- Farquhar, G.D., Ehleringer, J.R., Hubick, K.T., (1989). Carbon isotope discrimination and photosynthesis. *Annual Review of Plant Biology*, 40(1), 503-537.
- Fenton, J.H.C., and Smith, R.I.L. (1982). Distribution, composition and general characteristics of the moss banks of the maritime Antarctic. *Br. Antarctic Surv.*, 51, 215-236.
- Gavazov, K., Hagedorn, F., Buttler, A., Siegwolf, R., Bragazza, L. (2015). Environmental drivers of carbon and nitrogen isotopic signatures in peatland vascular plants along an altitude gradient. *Ecosystem Ecology*, doi: 10.1007/s00442-015-3458-4.

- Gonzalez-Zevallos, D., Santos, M.M., Rombola, E.F., Juares, M.A., Coria, N.R. (2013). Abundance and breeding distribution of seabirds in the northern part of the Danco Coast, Antarctic Peninsula. *Polar Research*, 32.
- Gorham, E. (1991). Northern Peatlands: Role in the carbon cycle and probable responses to climate warming. *Ecological Applications*, 1(2), 182-195.
- Huiskes, A.H.L., Boschker, H.T.S., Lud, D., Moerdijk-Poortvliet, T.C.W. (2006). Stable isotope ratios as a tool for assessing changes in carbon and nutrient sources in Antarctic terrestrial ecosystems. *Plant Ecology*, 182, 79-86.
- Jones, P.D., Marsh, R., Wigley, T.M.L., and Peel, D.A. (1993). Decadal timescale links between Antarctic Peninsula ice-core oxygen-18, deuterium and temperature. *The Holocene*, 3, 14-26.
- Keeling, R.F., Piper, S.C., Bollenbacher, A.F., and Walker, S.J. (2016). Flask Isotopic Data. [Monthly C13 concentrations from 1977 to 2013]. Retrieved from: <http://scrippsco2.ucsd.edu/data/spo>.
- Keeling, R.F., Piper, S.C., Bacastow, R.B., Wahlen, M., Whorf, T.P., Heimann, M., and Meijer, H.A. (2016). Flask CO<sub>2</sub> Data. [Monthly CO<sub>2</sub> concentrations from 1957 to 2015]. Retrieved from: <http://scrippsco2.ucsd.edu/data/spo>.
- Koning, Ross E. (1994). Bryophytes: Mosses. *Plant Physiology Information Website*. Retrieved from: [http://plantphys.info/plant\\_biology/copyright/moss.html](http://plantphys.info/plant_biology/copyright/moss.html).
- Koven, C.D., Ringeval, B., Friedlingstein, P., Ciais, P., Khvorostyanov, D., Krinner, G., Tarnocai, C. (2011). Permafrost carbon-climate feedbacks accelerate global warming. *PNAS*, 108(36), 14769-14774.
- Krupa, J. (1984). Anatomical structure of moss leaves and the photosynthetic rate. *Acta Societatis Botanicorum Poloniae*, 53, 43-51.
- Lee, Y., Lim, H.S., Yoon, H. (2009). Carbon and nitrogen isotope composition of vegetation on King George Island, maritime Antarctic. *Polar Biology*, 32, 1607-1615.
- Longton, R.E., (1988). *Biology of Polar Bryophytes and Lichens*. Cambridge University Press, Cambridge, England. 23-141.
- Mulvaney, R., Abram, N.J., Hindmarsh, R.C.A., Arrowsmith, C., Fleet, L., Triest, J., Sime, L.C., Alemany, O., Foord, S. (2012). Recent Antarctic Peninsula warming relative to Holocene climate and ice-shelf history. *Nature*, 489, 141-145.
- Moore, T.R., Roulet, N.T., Waddington, J.M. (1998). Uncertainty in predicting the effect of climate change on the carbon cycling of Canadian peatlands. *Climate Change*, 40, 229-245.

- Ochyra, R., Smith, R.I.L., Bednarek-Ochyra, H. (2008). *The illustrated moss flora of Antarctica*. Cambridge: Cambridge Press.
- Park, J-H., and Day, T.A. (2007). Temperature response of CO<sub>2</sub> exchange and dissolved organic carbon release in a maritime Antarctic tundra ecosystem. *Polar Biology*, 30, 1535-1544.
- Parnikoza, I.P., Convey, P., Dykyy, I., Trokhymets, V., Milinevsky, G., Tyschenko, O., Inozemtseva, D., Kozeretska, I. (2009). Current status of the Antarctic herb tundra formation in the central Argentine Islands. *Global Change Biology*, 15(7), 1685-1693.
- Peat, H.J., Clarke, A., Convey, P. (2007). Diversity and biogeography of the Antarctic flora. *Journal of Biogeography*, 34, 132-146.
- Proctor, M.C.F. (2005). Why do *Polytrichaceae* have lamellae. *Journal of Bryology*, 27, 221-229.
- Roberts, P., Newsham, K.K., Bardgett, R.D., Farrar, J.F., Jones, D.L. (2009). Vegetation cover regulates the quantity, quality and temporal dynamics of dissolved organic carbon and nitrogen in Antarctic soils. *Polar Biology*, 32, 999-1008.
- Robertson, S. (2011). Direct Estimation of Organic Matter by Loss on Ignition: Methods. *SFU*, 1-11.
- Royles, J., Ogee, J., Wingate, L., Hodgson, D.A., Convey, P., Griffiths, H. (2012) Carbon isotope evidence for recent climate-related enhancement of CO<sub>2</sub> assimilation and peat accumulation rates in Antarctica. *Global Change Biology*, 18, 3112-3124.
- Royles, J., Horwath, A.B., Griffiths, H. (2014). Interpreting bryophyte stable carbon composition: Plants as temporal and spatial climate recorders. *Geochem, Geophys, Geosys*, 15, 1462-1475.
- Royles, J., & Howard, G. (2014). Invited review: climate change impacts in polar regions: lessons from Antarctic moss bank archives. *Global Change Biology*, 21, 1041-1057.
- Royles, J., Amesbury, M.J., Roland, T.P., Jones, G.D., Convey, P., Griffiths, H., Hodgson, D.A., Charman, D.J. (2016). Moss stable isotopes (carbon-13, oxygen-18) and testate amoebae reflect environmental inputs and microclimate along a latitudinal gradient on the Antarctic Peninsula. *Global Change Ecology*, doi: 10.1007/s00442-01603608-3.

- Shevenell, A.E., Ingalls, A.E., Domack, E.W., Kelly, C. (2011). Holocene southern ocean surface temperature variability west of the Antarctic Peninsula. *Nature*, 252, 250-254.
- Silverside, A.J. (2010). Biodiversity reference. [Polytrichum commune]. Retrieved from: [http://bioref.lastdragon.org/Bryophyta/Polytrichum\\_commune.html](http://bioref.lastdragon.org/Bryophyta/Polytrichum_commune.html)
- Smith, R.C., Fraser, W.R., Stammerjohn, S.E. (2003). Climate variability and ecological response of the marine ecosystem in the western Antarctic Region. *Oxford University Press*, 10, 158-173.
- Stuber, S. (2013). The World of Mosses. *Arnoldia*. 71(1), 26-35.
- Stuiver, M., Reimer, P.J., Braziunas, T.F. (1998). High precision radiocarbon age calibration for terrestrial and marine samples. *Radiocarbon*, 40(3), 1127-1151.
- Thomas, R.J., Ryder, S.H., Gardner, M.I., Sheetz, J.P., Nichipor, S.D. (1996). Photosynthetic function of leaf lamellae in *Polytrichum commune*. *The Bryologist*, 99(1), 6-11.
- Thomas, E.R., Hosking, J.S., Tuckwell, R.R., Warren, R.A., Ludlow, E.C. (2015). Twentieth century increase in snowfall in coastal West Antarctic. *Geophysical Research Letters*, 42, 9387-9393.
- Turner, J., Colwell, S.W., Marshall, G.J., Lachlan-Cope, T.A., Carleton, A.M., Jones, P.D., Lugin, V., Reid, P.A., Igovkina, S. (2005). Antarctic climate change during the past 50 years. *Journal of Climatology*, 25, 279-294.
- Turney, C.S.M., Jones, R.T., Fogwill, C., Hatton, J., Williams, A.N., Hogg, A., Thomas, Z.A., Palmer, J., Mooney, S., Reimer, R.W. (2016). A 250-year periodicity in Southern Hemisphere westerly winds over the last 2600 years. *European Geosciences Union*, 12, 189-200.
- Zechmeister, H.G., Richter, A., Smidt, S., Hohenwallner, D., Roder, I., Maringer, S., Wanek, W. (2008). Total nitrogen content in  $\delta^{15}\text{N}$  signatures in moss tissue: Indicative value for nitrogen deposition patterns and source allocation on a nationwide scale. *Environmental Science & Technology*, 42, 8661-8667.